Science and Technology Facilities Council

Technical Report
STFC-TR-2026-001

Summary of space weather worst-case environments: (4th revised edition)

M Hapgood, R Horne, M Angling, et.al.

January 2026

Enquiries concerning this report should be addressed to:

RAL Library
STFC Rutherford Appleton Laboratory
Harwell Oxford
Didcot
OX11 0QX

Tel: +44(0)1235 445577
email: library@stfc.ac.uk

Science and Technology Facilities Council reports are available online at:
https://epubs.stfc.ac.uk

Accessibility: a Microsoft Word version of this document (for use with assistive technology) may be available on request.

DOI: 10.5286/stfctr.2026001

ISSN 2753-5797

Summary of space weather worst-case environments: (4th revised edition)

Version 6.1: 13 January 2026, coordinated by Mike Hapgood (mike.hapgood@stfc.ac.uk) and Richard Horne (rh@bas.ac.uk) on behalf of the UK Space Environment Impacts Expert Group

1 Scope of this document

1. Space weather may be described as **disturbances of the upper atmosphere and near-Earth space that disrupt a wide range of technological systems** – and, in a few cases, pose a direct threat to human health.

2. **The systems at risk are very diverse** and include power grids, GNSS, many aspects of spacecraft and aircraft operations, many types of radio communications and control systems.

3. **This note lists a number of these different systems** and outlines what we currently know of:
   - The space weather environment parameters that best summarise the threat to those systems;
   - A reasonable worst case for those parameters, together with the quality of the knowledge underpinning that estimate of the worst case and the formal provenance of that knowledge, e.g. in the peer reviewed literature;
   - What can be done to improve the quality of that knowledge;
   - Other useful information.

This information is presented in a series of tables – with each table focusing on a specific class of space weather threat to each particular system.

2 Context

1. The ultimate source of space weather is the Sun (see Appendix 1) and intervals of enhanced space weather risk are to some extent predictable, based on solar and geophysical observations. The **longest interval of severe space weather is likely to be of the order of two weeks,** based on the time it would take for a large region of activity on the Sun's surface to rotate across the Sun-Earth line [see, for example, the extreme event scenarios used in the impact studies by Eastwood et al (2018) and Oughton et al. (2018)].

2. During an interval of enhanced space weather risk, several different types of space weather can occur (see Appendix 1). The physical nature of space weather is extremely complex compared to terrestrial weather. This means that **during an interval of enhanced space weather risk, it is extremely difficult to predict the order, size, and duration of individual space weather phenomena.**

3. Therefore, different systems could experience adverse impacts (a) simultaneously, (b) sequentially, or (c) unpredictably (i.e., effectively randomly). Furthermore, **it is highly likely that these system failures will interact with each other** to cause cascading failure modes that are **fundamentally difficult to predict**.

3 Changes from the previous edition

This updates the summary of space weather worst case environments (3rd revised edition) that was published in January 2022, see https://doi.org/10.5286/raltr.2022001.

In this new edition the various severe space weather scenarios have been updated to include results from the UK's SWIMMR (Space Weather Instrumentation, Measurement, Modelling and Risk) programme that completed in 2024. These results include improved modelling of how geomagnetically induced currents (GIC) can impact the electricity transmission system in Great Britain, of how changes in the upper atmosphere affect satellites and space debris, of how changes in the ionosphere affect a range of radio technologies, and of how radiation environments in space and in Earth's atmosphere affect spacecraft and aircraft. These models are now being moved into operational use at MOSWOC, the Met Office Space Weather Operations Centre, together with use of new UK ground-based neutron monitors developed via the SWIMMR programme. SWIMMR has also supported the development of radiation monitors for use in aviation and on satellites.

The scenarios have also been updated to reflect experience gained during the severe geomagnetic storms that occurred in May and October of 2024. These provided an opportunity to review and improve our understanding of GIC impacts on the electricity transmission system as well as of satellite drag effects in low Earth orbit. The latter has highlighted that we need to better understand how such storms change the risk of collisions between satellites, especially in respect of the large constellations now present in low Earth orbit.

More broadly, this update also reflects improved modelling of GIC impacts on the Irish electric transmission system (which includes Northern Ireland). We also take account of recent results in assessing GIC impacts on the electricity transmission system in New Zealand, a small island system that is comparable to those in Great Britain and Ireland. The improved treatment of GIC impacts also reflects: (a) recent major advances in modelling GIC impacts on the DC track circuits used on many rail systems, and (b) a deeper assessment of GIC impacts on the transoceanic optical fibre cables that carry most intercontinental internet and telephone traffic.

Looking at non-GIC impacts, this update notes (a) how recent studies of cosmogenic isotopes in dateable materials (e.g. ice cores, tree rings) provide further evidence that, on thousand-year timescales, Earth is exposed to very severe radiation storms (often termed Miyake events) that would pose a serious hazard to aircraft and spacecraft, and (b) recent experimental studies have confirmed the theoretical assessment that solar radio bursts can interfere with mobile telephone reception when the phone's link to the base station is operating in marginal conditions. The scenarios have also been updated to provide an updated assessment of public behaviour in response to severe space weather, noting that the initial response is likely to be altruistic, but that this could be undermined by disinformation from social media and bad state actors.

Finally we note the scenarios have been updated to indicate where further work can advance our understanding of severe space weather and how to mitigate its adverse impacts, particularly via better forecasting that poses significant scientific challenges. In particular we note lessons learned from projects in the SWIMMR programme and from the recent advances in modelling impacts on rail systems.

4 Caveats

1. While this document provides separate descriptions of different space weather risks, it must be remembered that **many of these different risks will present themselves close together in time** – because they have a common origin in phenomena on the Sun. The associations between the different risks are illustrated in the figure at the end of this document.
2. This document focuses on the environmental aspects of space weather and **does not discuss measures that can be taken to provide resilience against space weather**, e.g. combined use of complementary technologies with different responses to space weather.

5 Contributors

Members of the UK Space Environment Impacts Expert Group: Mike Hapgood (RAL Space), Richard Horne (BAS) (Chair), Matthew Angling (U. Birmingham), Gemma Attrill (DSTL), Ciarán Beggan (BGS), Mario Bisi (RAL Space), Paul Cannon (U. Birmingham), Ellen Clarke (BGS), Clive Dyer (CSDRadConsultancy and U. Surrey), Jonathan Eastwood (Imperial College London), Sean Elvidge (U. Birmingham), Mark Gibbs (Met Office), David Gibbs (CAA), Lucie Green (MSSL), David Jackson (Met Office), Bryn Jones (SolarMetrics), Simon Machin (Met Office), Cathryn Mitchell (U. Bath), Matt Owens (U. Reading), John Preston (U. Essex), Graham Routledge (DSTL), Keith Ryden (U. Surrey), Harneet Sangha (UKSA), Rick Tanner (UK Health Security Agency), Jim Wild (Lancaster U.) and Mike Willis (UKSA).

6 Contents

7 Description of target risk impact tables

Each table is formatted as follow:

Target risk: NAMED RISK	
Environmental risk parameters:	A description of the way in which the environmental risk is quantified by either forecasters or system users.
Rationale:	An explanation of why the risk parameters are used in terms of the physical impact on the system.
Suggested worst case:	The most severe manifestation of the risk that can reasonably be projected to occur, based on peer-reviewed literature where possible. In line with wider risk planning, we have a strong focus on 1-in-100 years manifestations of the risk, but consider manifestations at longer timescales (e.g. 1-in-1,000 years) where there is good evidence of severe impacts. Note that the UK National Risk Assessment process originally considered risks from natural hazards that manifest above a likelihood of 1-in-100,000 years (Cabinet Office, 2017) but now has no formal lower limit, but assigns a low score to natural hazard risks that manifest with a likelihood of less than 1-in-2500 years (<0.2% in 5 years).
Worst case duration	The most severe duration that can reasonably be projected to occur, based on peer-reviewed literature where possible.
Worst case spatial extent	The geographic spread of the impact based on peer-reviewed literature where possible.
Anticipated effects	The likely impact on the system of the suggested worst-case risk, folding in the worst-case duration and spatial extent. It should be noted that the duration of the impact can be significantly longer than the duration of the space weather event.
Quality of case:	Evaluation of the quantity and depth of the peer reviewed literature and reports from professional/expert bodies that constitute the basis for the evaluation.
Provenance:	Key literature included in the reference list here that can be referred to for more detailed information.

Target risk: NAMED RISK	
How to improve case quality:	Expert group analysis describing where the impact case requires solidification or in many cases where the current state of the art lies. It should be recognised that space weather is a relatively new and evolving threat, because of scientific development, engineering development, and changes to the systems at risk that can make them both more and less exposed.
Other notes:	Other relevant information not covered elsewhere

8 Impact Tables

8.1 Electrical power transmission network

Target risk: Electrical power transmission network	
Environmental risk parameter:	Traditionally assessed (due to the broad time-span of geomagnetic records available) via time rate of change of magnetic field (d*B*/d*t*), specified in nano-Tesla per minute. However, risk assessment can also focus on the geoelectric field, *E*, as the primary geophysical risk parameter. In the UK, E-fields are particularly spatially complex, due to the underlying geology and surrounding seas, and this contrasts with some continental-scale nations. In the UK, both d*B*/d*t* and E-fields are relevant.
Rationale:	It has long been recognised that space weather poses a risk to the long-distance transport of electricity via the very high voltage (400, 275 and 132 kV) lines that form the transmission network across the UK (National Grid, 2021a; EirGrid, 2021). In particular, the risk is to the transformers that bind these lines into a network, and that link the network to electricity generators and distributors. Risk at transformer level is ultimately determined by the size of geomagnetically induced currents (GIC) flowing into and out of the transmission network, via transformer neutral connections, GIC depends closely on *E*, which, in turn, is induced by d*B*/d*t* in the conducting Earth. GIC also depends on line and earthing resistances within the transmission network, factors that are provided in the Electricity Ten-Year Statement (National Grid, 2021b). d*B*/d*t* is therefore a key source of GICs and directly drives *E*. But *E* also partly depends on (local/regional) ground conductivity and GIC also partly depends on grid electrical resistances and connectivity (e.g. Watermann, 2007, Cagniard, 1953, Hübert et al, 2025)
Suggested worst case:	For d*B*/d*t*, 5000 nT/min (one single event) is broadly consistent with the >95% upper confidence level in the Thomson et al (2011) 1-in-100 year scenario (the background level of the UK magnetic field is around 50,000 nT, for reference). Modelling work suggests a local peak geoelectric *E* field >20 V/km is typical of extreme event scenarios (e.g. 1 in 100 years or greater) in the UK (Beggan et al, 2013).

Target risk: Electrical power transmission network	
Worst case duration	Single event, or 'spike', in geoelectric field and d*B*/d*t* of 1-5 minutes duration. Lesser spikes (1-2 minutes each) will be observed frequently throughout the extreme event duration (hours to days). Historical occurrences of d*B*/d*t* >500nT/min have been associated with enhanced risk to the UK grid (e.g. Erinmez et al, 2002)
Worst case spatial extent	Growing evidence that intense GIC events have spatial scales of a few hundred km at most (Ngwira et al., 2015; Pulkkinen et al., 2015). Thus a single event would cover much of the UK. However it is important to appreciate that, during a severe geomagnetic storm, these intense GICs can occur anywhere in the UK, from Scotland to Cornwall, dependent on the orientation of the magnetic perturbations and the extent of the auroral oval. For example, post-event modelling of GICs in the GB transmission by Kelly et al. (2017) indicates that the largest GICs during the severe storm in March 1989 would have occurred at eastern and western edges of southern England and Wales, e.g. East Anglia, Cornwall, Pembrokeshire. This matches both (a) the experience reported by National Grid following that storm (Smith, 1990), (b) our modern understanding that a strong auroral electrojet in the ionosphere over southern England (as in March 1989, also May 2024), is likely to drive large GICs over the long east-west route (500 km) between East Anglia (e.g. Norwich) to western Cornwall. In summary, the key message is that the extreme GIC risk does not necessarily increase with latitude within the UK; in fact it may be the opposite due to intensification of the aurora as it moves southwards. It depends on details: the form of the magnetic perturbations, the regional and local ground conductivity, and the topology and resistances of the transmission network.

Target risk: Electrical power transmission network	
Anticipated effects	● Tripping of safety systems potentially leading to cascade failure of the transmission network and/or regional power outages. ● Transmission system voltage instability and voltage sag ● Possible premature ageing of transformers leading to decreased capacity in months/years following event (Gaunt, 2014). ● Damage, e.g. insulation burning, to a number of transformers, through transformer magnetic flux leakage. *(NB replacement of a transformer can take 1 to 2 months if a spare is available elsewhere in the UK; and much longer if procurement of a new transformer is required. NESO now holds an increased number of spares to account for this risk across Great Britain.)*
Quality of case:	Kappenman (2006) paper: Based on a single measurement of earth currents on a railway circuit in central Sweden during May 1921. Calibrated by linear extrapolation from similar but smaller earth currents observed in Sweden during a 2500 nT/min event in 1982. Thomson et al (2011) paper: Published extreme event value statistical analysis of 1982-2010 digital magnetometer data from northern Europe. Similar results obtained in extreme event value analyses for Canada (Nikitina et al., 2016) and northern Europe (Wintoft et al., 2016), and a recent more detailed analysis for the UK (Rogers et al., 2020)
Provenance:	Peer-reviewed papers by Kappenman (2006) Thomson et al. (2011), Rogers et al. (2020).. See also papers by Beggan et al (2013), Kelly et al (2017) and Hübert et al (2025) for UK hazard in terms of GIC and electric fields.

Target risk: Electrical power transmission network	
How to improve case quality:	Initial work on the following topics has been started and has informed our understanding of the top level risk. The detailed evaluation of the risk at the substation and transformer level can be improved with additional research: ● Further analysis of UK geomagnetic observatory data running from the 1850s to 1982 (digitised paper records) and 1983-2012 (measured digital data) to determine spatial structure and correlations during extreme events. Paper records could be digitised to allow digital analysis of older storms. ● Better characterisation of UK ground conductivity to enable improved modelling of geoelectric fields using denser magnetotelluric surveying of the UK. ● Better understanding of the spatial and temporal scales of dB/dt arising from sub-storms ● Industry GIC measurements in substations and their correlation with changes in the geomagnetic data would stimulate development and validation of models of the hazard. This could be in conjunction with NESO or SPEN ● Characterisation of the spectrum of B, dB/dt and geoelectric field E during extreme storms, e.g. to determine magnitudes and numbers of peak and any lesser spikes as well as expected occurrence rates. There is emerging evidence of potential impacts on other systems such as the lower voltage distribution networks that receive electrical power from the transmission network and deliver it to end users. We discuss this further in section 8.1.

Target risk: Electrical power transmission network	
Other notes:	● The largest recorded disturbance of the last 40 years was around 2700 nT/min, measured in southern Sweden in 1982. The largest UK disturbance was 1100 nT/min at Eskdalemuir in March 1989. ● Key impacts of the March 1989 storm on the national grid in England and Wales were reported by Smith (1990) with more detail now reported by Boteler (2019). ● Modelled GIC and surface electric fields suggest a per substation GIC of 10s to 100s of amps and local peak electric fields of ~25 V/km for Carrington scale events (c. 1 in 200 years) is possible (e.g. Pulkkinen et al, 2015; Ngwira et al, 2013; Beggan et al, 2013; Kelly et al., 2017) ● Studies of GIC in the Irish power grid (which serves both Northern Ireland and the Irish Republic) have been published by Blake et al. (2017 and 2018) and updated by Malone-Leigh et al (2024) ● The May 2024 storm was a test of the work and research developed during the NERC highlight project SWIGS, and during the SAGE project that was part of the SWIMMR programme. It was a 'low' G5 event which Lawrence et al (2025) describe in detail. It had no damaging effects on the GB power grid. ● The recent and extensive studies on the New Zealand grid (Rodger et al., 2017 and 2020; Divett et al., 2017; Mac Manus et al., 2017; Clilverd et al., 2018, Mac Manus et al, 2022 and 2023), an island nation with similar magnetic latitude to the UK, suggest the maximum GIC could reach 600 amps for a 1-in-100 year event. ● For context, the Dst index (an equatorial measure of the magnetospheric ring current) reached -589 nT in March 1989. The Dst of the Carrington event was estimated as -1760 nT (Tsurutani et al, 2003), but more recent work (Siscoe et al., 2006; Cliver and Dietrich, 2013) suggests a value between -850 and -1050 nT, with a recurrence likelihood of 3-12% per decade (e.g. Riley, 2012; Love, 2012; Riley and Love, 2017, Hayakawa et al, 2024, Love et al, 2025).

8.2 Satellite operations – electronic component ageing and solar array degradation (cumulative radiation effects)

Target risk: Satellite operations –cumulative radiation effects	
Environmental risk parameter:	Cumulative damage (ageing) is due to the deposition of energy or 'dose' into materials due to both the electron and proton environments. While this dose accumulates over the whole satellite lifetime, an extreme event would cause a more sudden ageing effect which could be significant. Thus solar proton fluence and energy spectrum, as well as radiation belt energetic electron and proton fluences and energy spectra are the key parameters. As a result the worst case will be orbit dependent as we discuss below. Lower energy protons (1 to 10 MeV) and medium energy electrons (0.1 to 1MeV) are the most relevant for solar array damage, while higher energies of both species penetrate to internal electronic components. For electrons, the relevant population is essentially the same as that which causes internal charging (see section 4). The ionising element of dose is usually measured in rads (1rad = 0.01Gy). The non-ionising dose element (also called displacement damage) is measured by the equivalent damage fluence of 10 MeV protons or 1 MeV electrons, or by the Non-Ionising Energy Loss (NIEL) in MeV/g or J/kg. Electrons and protons contribute to both elements of the dose.
Rationale:	Modern digital metal-oxide semiconductor (MOS) electronic technology is mainly damaged by ionising dose. Bipolar (primarily analogue) electronic devices can be strongly affected by non-ionising dose (displacement damage): included in this category is loss of solar cell efficiency. However many bipolar devices can also be damaged by ionising dose. Depending on the orbit, energetic electrons can be more important than protons for solar array damage (Hands et al., 2018).

Target risk: Satellite operations –cumulative radiation effects	
Suggested worst case:	Protons, >1 MeV (for solar array damage): 1.3 x10^{11} $cm^{-2;}$ Protons, >30 MeV (for ageing of internal components): 1.3 x 10^{10} cm^{-2} both from Xapsos et al., 1999 & Xapsos et al., 2000 Electrons: > 2 MeV as for internal charging with fluence integrated over 1 week; i.e. 4.4x10^{11} $cm^{-2}sr^{-1}$ for 1-in-100, 1x10^{12} $cm^{-2}sr^{-1}$ for 1-in-150 year event based on GOES-West. Would be a factor 1.11 worse at worst GEO longitude of 160°W according to the AE8 model (Vette, 1991) and 1.04 according to the AE9 model (Ginet et al., 2013). See the discussion below showing how the worst case varies with type of orbit (GEO, MEO and LEO) and location around that orbit in the case of GEO. (N.B. see the glossary for an explanation of orbit acronyms.)
Worst case duration	Protons: Single event lasting 2 days or series of events lasting 1 week. Electrons: one week enhancement (see discussion under internal charging) For worst case a severe electron enhancement would probably follow after the severe proton event so both events need consideration together: the electron enhancement may be the more damaging (Ryden et al., 2008; Hands et al., 2018).
Worst case spatial extent	Most satellite orbits are exposed; the magnetosphere will provide shielding from solar energetic particles for some orbits, especially equatorial LEO. Electrons dominate this impact for MEO satellites, and have an impact comparable with solar protons for GEO satellites.
Anticipated effects	Premature ageing (potentially by some years) of spacecraft electronic components, including solar arrays, leading to decreased capacity following the event and/or reduced lifetime. See Hands et al (2018) for examples.
Quality of case	We refer to ECSS-E-ST-10-04C Rev.1 for our current worst case event which is based on extrapolating existing models.
Provenance:	ECSS-E-ST-10-04C Rev.1 standard. Also papers by Xapsos et al. (1999), and Xapsos et al. (2000).

Target risk: Satellite operations –cumulative radiation effects	
How to improve case quality:	● Continue to monitor work on proxy data such as ^{14}C and ^{10}Be studies (Miyake et al, 2012; Mekhaldi et al., 2015, O'Hare et al., 2019), especially efforts to derive energy spectra and to improve time resolution of historical events, such as 774AD. The subject has recently been reviewed in Miyake, Usoskin, Poluianov et al. (2020). NB We note Brehm et al. (2021) have recently identified additional historical events in 7176 and 5259 BCE. Bard et al (2023) identified strongest known cosmogenic SEP event in 14,300 BP (12,350 BCE) and Golubenko et al (2025) have calculated >200 MeV fluence of the event as 1.4 $x10^{10}$ cm^{-2}. This is 18% stronger than 775CE/AD which is within error for existing estimates. ● These new results provide further evidence in support of the worst case presented here. ● In addition, the NERC-funded Satellite Radiation Risk Forecasts (Sat-Risk), part of the SWIMMR programme running from 2020 to 2023, has developed a real-time system to forecast radiation exposure to satellites for a range of different orbits to help quantify the risk of damage or degradation. This is in the process of being made operational at MOSWOC.
Other notes:	Damage depends on the energy spectrum. Internal components suffer more from hard spectra. For solar cells, damage is more severe for soft spectra. Further investigation of models is needed, e.g. SAPPHIRE (Jiggens et al, 2018).

8.3 Satellite operations – Single Event Effects/control

Target risk: Satellite operations – SEE/control	
Environmental risk parameter:	Solar energetic proton flux and fluence (> 30 MeV). Heavy ions also contribute to SEEs and can double the rates calculated from protons alone (Dyer et al., 2004). In addition, heavier ions can give hard failures not produced by protons.
Rationale:	The rate at which SEEs occur is related to this flux but depends on the hardness of the spectrum and the amount of shielding. Thus the frequency of service interruptions, and the size of operator workload, in any period, will also rise and fall with this flux. The fluence over a day is a useful guide to the total number of problems to be expected.
Suggested worst case:	Peak proton flux, >30 MeV: 3.8 x 10^5 $cm^{-2}s^{-1}$, 1-day proton fluence, >30 MeV: 6.8 x 10^9 cm^{-2} , 1-week proton fluence, > 30 MeV: 1.6x10^{10} cm^{-2} all with the energy spectrum as in October 1989 or August 1972. Based on values derived from the Creme96 model by Dyer et al. (2004) and multiplied by four to estimate the 1-in-150 year event. The Creme96 model is based on high-energy particle observations during the extreme SEP events of October 1989. For 1-in-100 year event the estimate is 2.4 times the Creme96 values giving Peak proton flux, >30 MeV: 2.3x10^5 $cm^{-2}s^{-1}$, 1-day proton fluence, >30 MeV: 4.1x10^9 cm^{-2} , 1-week proton fluence, > 30 MeV: 1.0x10^{10} cm^{-2} Cliver and Dietrich (2013) estimate a fluence between 10^9 and 10^{11} cm^{-2} >30 MeV for a 1-in-150 year event, with a best estimate of 1.1x10^{10} cm^{-2}. But this is based on the Carrington event of 1859 and assumes a correspondence between geomagnetic storms, flare size and SEP events that is now thought doubtful (Owens et al., 2022). For now rates can be doubled to allow for ions.
Worst case duration	1-2 days for each event, but there could be several lasting a week as in October 1989 and October 2003.
Worst case spatial extent	Most satellite orbits are exposed: the magnetosphere will provide shielding for some orbits, especially equatorial LEO. We do not consider the South Atlantic Anomaly here as that is a slowly varying feature that will cause SEEs when satellites cross that region, irrespective of solar events.

Target risk: Satellite operations – SEE/control	
Anticipated effects	High anomaly rates on spacecraft: ● High workload by spacecraft operators to restore nominal spacecraft behaviour ● Temporary reduction in capacity of spacecraft services ● Some potential for permanent loss of sub-systems and of the whole spacecraft.
Quality of case:	Based on extrapolation from space age measurements. This may be supplemented in future by use of cosmogenic isotopes to estimate historical SEP events; this is an area of ongoing research.
Provenance:	Dyer et al., 2004.
How to improve case quality:	Improved understanding of SEP events as discussed above and inclusion of worst case fluences from ions and their Linear Energy Transfer (LET) spectra. Dyer et al (2004) shows that Creme96 is a reasonable worst-case LET spectrum for the space age, but a 1-in-150 year event might well be factor 4 worse as with the proton estimates.
Other notes:	Depends on the energy spectrum of the particles. Probably most severe for intermediate hardness. Suggest use October 1989 or August 1972 to enable scaling from existing space standards- maybe by factor 4 for 1 in 150 years. Also need to assume worst case composition for heavy ions.

8.4 Satellite operations – internal charging

Target risk: Satellite operations – internal charging	
Environmental risk parameter:	Energetic electron flux (~0.5 to 10 MeV) It is important to consider the electron spectrum. The electron flux >2 MeV is often used as the measure of risk. The minimum energy depends on the level of shielding around sensitive components. Significant flux >6 MeV has been observed by Van Allen Probes.
Rationale:	These very energetic electrons penetrate deep inside spacecraft. Thus electrical charge can accumulate in dielectric (electrically insulating) materials. If this accumulation becomes too large, the dielectric will break down resulting in an electrical discharge. This can (a) damage nearby spacecraft systems, and (b) generate false signals that cause the spacecraft to misbehave. The latter will drive up operator workload.
Suggested worst case:	This depends on electron energies and orbit location as follows (see the spatial extent section for how to adjust to other longitudes). **Geosynchronous orbit**: ● 1 in 100 year daily average flux of E > 2 MeV electrons at GOES West is 7.7×10^5 $cm^{-2}s^{-1}sr^{-1}$ [*Meredith et al*., 2015]. 1 in 100 year flux of electrons in the energy range 0.69-2.05 MeV at L* = 6.0 in the near equatorial region (-15° < magnetic latitude < 15°), representative of geosynchronous orbit ranges from 4.7×10^6 $cm^{-2}s^{-1}sr^{-1}MeV^{-1}$ at 0.69 MeV to 1.6×10^5 $cm^{-2}s^{-1}sr^{-1}MeV^{-1}$ at 2.05 MeV. A spectrum of worst cases is available at 10 energies in the range 0.69-2.05 MeV. [*Meredith et al*., 2017]. ● [*Meredith et al, 2023*] provide a further 1-in-100 year differential flux spectrum for L=6.5 and a max. limiting flux for 0.6 MeV (above this energy the fluxes appear unbounded). **Medium Earth orbit (e.g. for GPS and Galileo)**: ● 1 in 100 year flux of electrons in the energy range 0.69-2.05 MeV at L* = 4.5 in the near equatorial region (-15° < magnetic latitude < 15°), representative of the peak fluxes encountered in GNSS type orbits, ranges from $1.5 \times 10^7 cm^{-2}s^{-1}sr^{-1}MeV^{-1}$ at 0.69 MeV to 5.8×10^5 $cm^{-2}s^{-1}sr^{-1}MeV^{-1}$ at 2.05 MeV [*Meredith et al*., 2017]. ● 1 in 100 year daily average internal charging current, averaged along the orbit path, behind 1.5 mm of aluminium is 1.3×10^{-13} A cm^{-2} [*Meredith et al*., 2016a] which exceeds the NASA guidelines

Target risk: Satellite operations – internal charging	
	of 1 x 10^{-13}A cm^{-2} over a 10 hour period [*NASA,* 2011] ● Also [*Meredith et al, 2023*] provide a further 1-in-100 year differential fluxes for L=4.5 as well as max. limiting fluxes up to 2 MeV. The max. flux at these energies appears bounded (saturated). **Low Earth orbit: 800 km altitude.** ● 1 in 100 year flux of E >300 keV electrons shows a general decreasing trend with L*, ranging from ~10^7 $cm^{-2}s^{-1}sr^{-1}$ at L* = 3x10^5 $cm^{-2}s^{-1}sr^{-1}$ at L* = 8.0 [*Meredith et al.,* 2016b]. *NB. L* is the invariant coordinate developed by Roederer for radiation belt studies (Roederer, 1970; Roederer and Lejosne, 2018).*
Worst case duration	2-5 days
Worst case spatial extent	Peak fluxes vary with longitude around the geostationary ring, because magnetic latitude also varies around the ring. Worst case GOES $E > 2$ MeV flux above is for the GOES West location (135°W). The 1 in 100 year $E > 2$ MeV flux at the GOES East location (75° W) is a factor of 2.4 less than that at GOES West (Meredith et al., 2015). Using the AE8 average model, the UK longitude at 0°E has only slightly lower flux (by about 10%) than that at 20°E which is the local maximum in the European region. Note however that fluxes higher than those at 20°E occur at longitudes from approximately 170°E to 230°E (130°W). Using AE9 gives different factors.
Anticipated effects	High anomaly rates on spacecraft: ● High workload by spacecraft operators to restore nominal spacecraft behaviour ● Temporary reduction in capacity of spacecraft services Some permanent damage from electrostatic discharges is also possible. ● Worst case internal charging effects analysis given in Horne et al. (2025).
Quality of case:	Recent peer reviewed papers by Meredith et al, 2015, 2016a, 2016b, 2017 and 2023 give robust extremes. These fluxes are consistent with earlier theoretical estimates [Shprits, 2011; O'Brien et al, 2007].
Provenance:	Peer reviewed papers by Meredith et al (2015, 2016a, 2016b, 2017, 2023), O'Brien et al., (2007) and Shprits et al., 2011)

Target risk: Satellite operations – internal charging	
How to improve case quality:	● More testing and verification of the BAS-Radiation belt model (BAS-RBM) against satellite data for LEO, MEO, and GEO ● Observations of electron flux between 1,300 km and 20,000 km altitude along the magnetic equator where there are no in-situ data and thus must rely on models. ● Development of storm-time wave-particle interaction models to better capture the variability during major storms ● Coupling of the solar wind data and models to the BAS-RBM to improve the forecasting chain. ● More in-orbit measurements of internal charging currents and effects: SWIMMR funded a small project to advance the UK SURF internal charging instrument and ESA has also placed the ASPIRE project with similar aim.
Other notes:	Radiation-induced conductivity can help to mitigate internal charging by increasing the rate at which charge leaks out of dielectric materials in satellites (Ryden and Hands, 2017)

8.5 Satellite operations – surface charging

Target risk: Satellite operations – surface charging	
Environmental risk parameter:	Electron flux (1 to 100 keV) It is important to consider the electron spectrum. The worst-case spectrum from SCATHA was mostly enhanced above the average between 20 - 100 keV.
Rationale:	The surfaces of objects in space always acquire some electrical charge. In strong sunlight, this is usually dominated by photoemission from the object, which stabilises the electrical potential at a few volts positive. But in regions of space containing hot plasmas, especially outside sunlight, the surface can go to a negative potential of several thousand volts. If this potential becomes too large it may trigger an electrical discharge. This can (a) damage systems on the spacecraft surface (e.g. solar arrays), and (b) generate false signals that cause the spacecraft to misbehave. The latter will drive up operator workload. Surface charging often occurs: ● As a satellite passes out of eclipse into sunlight, due to change in currents to & from the spacecraft ● During substorms which inject typically 1 – 100 keV electrons across geosynchronous and medium Earth orbit, usually between midnight and dawn (O'Brien, 2009). ● During intense aurora caused by 1-10 keV electrons which affect satellites in polar low Earth orbits crossing the auroral regions Surface charging is determined by the flux of electrons in the hot plasma in these regions.
Suggested worst case:	Typically a peak electron flux of 10^7 cm^{-2} sr^{-1} s^{-1} keV^{-1} at 30 keV and 3 x 10^6 cm^{-2} sr^{-1} s^{-1} keV^{-1} at 100 keV where the SCATHA worst case flux exceeds the average most (Fennel et al., 2001) and also Mateo-Velez et al. (2018).
Worst case duration	Substorms causing plasma injections may last several mins after which the peak flux will decay. However, during active periods multiple substorms occur with an interval of one to a few hours between each substorm. Prolonged periods of multiple substorms can last for 10 days or more during high speed solar wind streams.
Worst case spatial extent	Needs further study

Target risk: Satellite operations – surface charging	
Anticipated effects	Permanent damage to spacecraft systems, particularly solar arrays. High anomaly rates on spacecraft: ● High workload by spacecraft operators to restore nominal spacecraft behaviour ● Temporary reduction in capacity of spacecraft services
Quality of case:	Surveys of publicly available measurements.
Provenance:	Analysis of GEO data (Fennel et al., 2001; Mateo-Velez et al., 2018)
How to improve case quality:	Further survey of available datasets & the published literature, especially new papers that address the issue.
Other notes:	

8.6 Satellites – Thermospheric Drag

Target risk: Satellites – Thermospheric Drag	
Environmental risk parameter:	Change in thermospheric neutral density below 1,000 km satellite orbit altitude
Rationale:	Density changes affect satellite orbital determination, since they lead to changes in the drag on the satellite
Suggested worst case:	Observed relative density enhancements of up to 800% (Liu and Lühr, 2005). Model simulation suggests density enhancements of over 1400% for a 1 in 100 year extreme event, but this result has a high uncertainty (estimated to be 100%). Absolute density changes of up to at least 5 x 10^{-12} kg m^{-3} (at 500 km altitude), as observed during the October 2003 storms (Krauss et al., 2015).
Worst case duration	Large changes described above take place within a few hours. Worst-case storm disturbances can last on the order of days if multiple CMEs strike in succession. Typically, the thermosphere recovers to near pre-storm density levels within ~1–3 days. Enhanced infrared cooling (primarily via nitric oxide emission) in the aftermath can accelerate the decline in density. A phenomenon known as “thermospheric overcooling” has been observed after some intense storms: the density can briefly drop below the original quiet-time baseline due to strong radiative cooling (pre-storm level decreases of 23% were observed after the May 2024 storm (Ranjan et al., 2024)).
Worst case spatial extent	Effects likely all over the world. Geomagnetic storm heating is heaviest in the high-latitude auroral regions (where energetic particles and Joule heating dump energy into the atmosphere). From there, the effects propagate globally through atmospheric waves and winds. Large-scale atmospheric gravity waves known as Travelling Atmospheric Disturbances (TADs) carry the density enhancements equatorward. Observations and models show that the thermospheric response spreads remarkably fast: typically within 1–2 hours the mid-latitudes are affected, and within ~3–4 hours even low-latitude (near-equatorial) regions feel the density increase (Oliveira et al., 2017; Sutton et al., 2009). By a few hours into the storm, the thermospheric expansion is a planet-wide phenomenon (though still greatest near the auroral zones). This means satellites in all inclinations, not just polar or high-latitude orbits, will experience increased drag within hours of storm onset. There is also some asymmetry and local time dependence (e.g. nightside vs dayside differences), but the overall response envelops the entire LEO environment quickly.

Target risk: Satellites – Thermospheric Drag	
Anticipated effects	● Satellite loses altitude, or satellite raising manoeuvres need to be carried out to counteract this. Examples: ▪ NOAA SWPC estimated the ISS would drop by 200 m in a day during the October 2003 Halloween storm, but by 45 m in a day on a non-stormy day during the same month. ▪ KANOPUS-V3 (~500 km) saw its decay rate jump from ~38 m/day (in quiet conditions) to ~180 m/day during May 2024 (Parker & Linares, 2024) ▪ CHAMP (GRACE) drops in satellite altitude by 90-120 m (40-50 m) (Krauss et al, 2018) during extreme CMEs ● Spacecraft in many modern satellite constellations will manoeuvre autonomously to counteract drag effects. This will challenge systems that track and maintain awareness of satellite positions. This en-masse raising of orbits is unprecedented in earlier eras; for comparison, during the 2003 storms virtually no satellites performed immediate orbit corrections, as few had autonomous drag compensation then. ● During the very large geomagnetic storm of 13-14 March 1989, tracking of thousands of space objects was lost and it took North American Defense Command many days to reacquire them in their new, lower, faster orbits (Berger et al., 2023). Berger et al (2020) indicated an increase of cumulative positional error during even moderate geomagnetic storms at 500-600 km orbital altitude of up to 500-700m if the storm is of 3 hrs duration, and up to 7 km if the storm lasts for 18 hours. ● These changes due to density variations are dependent on altitude and on spacecraft size, shape, and orientation. ● The drops in orbital altitude can also lead to premature re-entry for satellites already close to end of life (e.g. the Student Nitric Oxide Explorer during the 2003 Halloween Storm). ● Issues with orbital determination – in extremis satellites have crashed into each other ● Tracking of space debris is made significantly more problematic ● Premature re-entry of satellites launched into very low (~200 km) initial orbits during periods of geomagnetic activity, e.g. the loss of 38 Starlink satellites in February 2022 (Hapgood et al., 2022)

Target risk: Satellites – Thermospheric Drag	
Quality of case:	Observed worst case based on 2003 to 2015 period. Model simulation of a 1 in 100 year event contains uncertainties but is usable as a guide. Extending model simulations to theoretical worst case is not yet possible without further research.
Provenance:	Krauss et al. (2015, 2018) – density fluctuations observed by CHAMP and GRACE during geomagnetic storms from 2003-2015; Sutton et al (2005) - density fluctuations observed by CHAMP in October 2003 geomagnetic storms. Reeves et al. (2019),- thermospheric response to increase in EUV over a period of at least 1 day Le et al. (2016) – thermospheric response to theoretical strongest solar flares. Oliveira et al. (2017) – shows how thermospheric response spreads from high to low latitudes following geomagnetic activity. Oliveria and Zesta (2019) - investigates the effects caused by atmospheric drag forces on satellites orbiting between ~300- to 500-km altitude during a range of geomagnetic storms. Bruinsma et al. (2023) - provides a comprehensive review of current capabilities in thermosphere and satellite drag modelling, specification and lists recommendations.
How to improve case quality:	▪ Further exploitation of satellite accelerometer data, including assimilation of such data into models. ▪ A general improved understanding of the interactions between extreme forcing and the thermosphere, so that key parts of models are based on physical understanding rather than being based on observations (which cannot represent the most extreme events). A particular focus on improving knowledge of saturation of magnetospheric forcing on the thermosphere and ionosphere is needed. ▪ An improved understanding of how satellite collision risks will evolve due to storm-driven changes in drag ▪ Extreme value analysis of theoretical absolute and relative changes in neutral density ▪ Exploitation of observations of satellite orbit changes, including premature re-entries, during recent major storms in May (Gannon) and October 2024 (e.g. Parker & Linares, 2024; Oliveira et al., 2025).

Target risk: Satellites – Thermospheric Drag	
Other notes:	Enhancement of EUV on timescales of greater than 1 day and associated with strong solar active regions can lead to neutral density increases, for a theoretical worst case, of 105% at 250 km and 165% at 400 km (Reeves et al., 2019). Transient density increases above quiet conditions due to an assumed theoretical maximum solar flare (with associated short term enhancement of EUV) can be as high as 20% at 200 km, 100% at 400 km and 200% at 600km (Le et al., 2016). Density changes due to High Speed Solar stream (HSS)-driven storms are similar in magnitude to those due to CME-driven storms, apart from those related to strongest ~10% of CME-related storms (Krauss et al, 2018). Note that the HSS-driven storms are often of longer duration than the CME-driven storms. Accordingly, the integrated effect of many such small storms, or flares, on satellite orbits may also need to be examined. The impact of anticipated effects is likely to increase in future due to increasing space debris and proposed constellations of hundreds of nanosatellites. We need to better understand implications for satellite survey and tracking.

8.7 Terrestrial Electronics

Target risk: Terrestrial Electronics	
Environmental risk parameter:	Cosmic ray neutron flux (>10 MeV) at Earth's surface
Rationale:	Secondary neutrons are the dominant source of single event effects below 60000 feet and are produced when energetic protons and ions from space interact with nitrogen and oxygen nuclei in the atmosphere. The flux > 10 MeV is used in the standards but allowance must be made for lower energy neutrons, especially thermal. Note that energetic protons can contribute significantly while for new technologies stopping protons and muons are increasingly significant.
Suggested worst case:	For a 1-in-150 year event, 200-fold increase in surface radiation environment for latitudes such as London, UK. For a 1-in-100 year event the estimated increase is a factor 120. This is based on a recent assessment of extreme events by Dyer et al. (2017). Using both the ground level radiation monitor records and proxies such as ^{14}C and ^{10}Be, this assessment suggests to use a 1-in-150 year worst case that is 4 times more intense than the largest event observed with instruments (a 50-fold increase measured at Leeds on 23 Feb 1956). For 1-in-150 year event, sea level neutron fluxes > 10 MeV are: ● $2.1x10^3$ $cm^{-2}hr^{-1}$ at London ● $1.1x10^4$ $cm^{-2}hr^{-1}$ for North of Scotland For 1-in-100 year event these fluxes become: ● $1.3x10^3$ $cm^{-2}hr^{-1}$ at London ● $6.6x10^3$ $cm^{-2}hr^{-1}$ for North of Scotland For higher latitudes there is essentially no geomagnetic shielding. This assessment also suggests the 1-in-1000 year worst case would be a 1000-fold increase in the surface radiation environment at London and 5000-fold for the North of Scotland. For more detail see the tables in Dyer et al. (2017)
Worst case duration	Timescales of events range from 1 to 12 hours but note that for impulsive events such as Feb56, nearly all the fluence (77%) arrives in the first hour and fluxes during the first few minutes are a factor 3 higher.,

Target risk: Terrestrial Electronics	
Worst case spatial extent	Considerable variations across the world due to radiation from the Sun being directed by the interplanetary magnetic field, and the shielding effects of Earth's magnetosphere. The former can lead to variations with longitude, whilst the latter can lead to greater fluxes at high latitudes – but with marked differences between the northern and southern poles. If a ground level enhancement occurs during an extreme geomagnetic disturbance, such as that during the Carrington event, low latitudes could be severely exposed.
Anticipated effects	Greatly enhanced error rates in unprotected digital electronic systems, also potential for damage to such devices and burnout in high voltage devices (see Box 2 in Cannon et al. (2013),also discussion in Dyer et al. (2017) and Dyer et al. (2020)). A particular concern here is the impacts on electronic control systems used in the nuclear power sector, where there is a requirement to consider and mitigate the risks that could arise from very rare (1-in-10000 years) events of any kind (HSE, 1992). This concern has prompted industry to engage with researchers to assess the problem, e.g. as in Taylor (2013) and Dyer et al. (2020).
Quality of case:	This is based on observations of the ground level enhancement (GLE) radiation event of 23 Feb 1956 and comparison with other GLEs in the instrumental and proxy records, as consolidated by Dyer et al., 2017.
Provenance:	Marsden et al (1956), Quenby and Webber (1959), Rishbeth, Shea and Smart(2009), Tylka and Dietrich (2009), Mekhaldi et al. (2015), Dyer et al. (2017).
How to improve case quality:	Further work on cosmogenic nuclides and co-ordinated observations of future GLEs across a wide range of locations and altitudes. Bard et al (2023) identified strongest known cosmogenic SEP event in 14,300 BP (12,350 BCE) and Golubenko et al (2025) have calculated >200 MeV fluence of 12,350 BCE as 1.4 x10^{10} cm^{-2}. This is 18% stronger than 775CE/AD but within error on existing estimates.

Target risk: Terrestrial Electronics	
Other notes:	February 1956 is the most severe event observed since observations commenced in 1942. The Carrington event itself does not appear to have been a severe event as it is not seen in the cosmogenic nuclide records. However, the analysis by Dyer et al. shows that events four times larger than the February 1956 event occur approximately every 150 years on average. Evidence from the AD774 event suggests that this event was very severe. Effects are probably worse for short events that give high flux rates. Event durations are typically 1-12 hrs. Dyer et al. (2017) propose adoption of a new space weather scale for atmospheric radiation with February 1956 fluxes as the baseline for the scale and with scaling measurements obtained from ground-based neutron monitors. The low energy neutron spectra at ground level are greatly influenced by local conditions such as soil moisture and precipitation. This can be important if components are sensitive to low energy neutrons (< 10 MeV) and/or to thermal neutrons. For neutron monitoring at nuclear reactor or fuel processing sites care must be taken to distinguish increases due to GLEs from those due to a criticality accident.

8.8 Radio technologies

Target Risk: Radio technologies	
Environmental risk parameter:	Solar radio flux
Rationale:	The Sun can produce strong bursts of radio noise over a wide range of frequencies from 10 MHz to 10 GHz. These bursts may interfere with radio systems operating at these frequencies if the solar signal is stronger than the operational signal. This will arise, in particular, where it is necessary to detect relatively weak radio signals, e.g. GNSS receivers; radars; base station reception of signals from mobile phones; VHF, UHF and L-band satellite communications. For avoidance of doubt, we note that the Sun can produce strong radio bursts at frequencies below 10 MHz, but these are usually blocked by the ionosphere. Thus, they do not interfere with ground- and aircraft-based radio systems working at lower frequencies.
Suggested worst case:	2×10^{-16} W m^{-2} Hz^{-1} (2 million SFU) over a broad range of frequencies. (Taken as twice the worst observed case from Dec 2006, as noted below.)
Worst case duration	1 hour
Worst case spatial extent	Whole dayside of the Earth.
Anticipated effects	Interference can disrupt operation of vulnerable radio systems, with the form of the disruption dependent on the system design and configuration. This is a natural jamming process.
Quality of case:	Statistical studies show that radio bursts up to 10^{-17} W m^{-2} Hz^{-1} are fairly common. A burst of 10^{-16} W m^{-2} Hz^{-1} was recorded in Dec 2006 and disrupted GNSS systems across the sunward side of the Earth (Cerruti et al., 2007). In November 2015, a burst in excess of 10^{-17} W m^{-2} Hz^{-1} disrupted aircraft control radars in Belgium, Estonia and Sweden (Marqué et al., 2018).
Provenance:	Statistics in peer-reviewed paper by Nita et al. (2004). Impact analyses by Cerruti et al. (2007) and Marqué et al. (2018). Observed solar interference in Italian mobile networks (Muratore et al., 2022).
How to improve case quality:	Conduct extreme value analysis to determine reasonable worst case and assess in light of wireless system operating parameters.

Target Risk: Radio technologies	
Other notes:	The potential for radar disruption by solar radio bursts has been known since 1942 (Hey, 1946). So, this disruption is generally well-mitigated by good design and operational procedures. However, the November 2015 event cited above shows a need to maintain awareness. For mobile cellular systems, SRBs with energy flux 10^{-17} W m^{-2} Hz^{-1} should just be detectable by mobile phones. For base stations, the effect will be greatest at sunrise/sunset when the Sun lies in the base station antenna beams. A recent study on Italian networks (Muratore et al., 2022) has demonstrated this effect in a case study of radio bursts disrupting mobile services operating in marginal conditions, e.g. weak signals due to distance from the base station. The impact on satellite communications will be most significant for geostationary satellites around equinox, when the satellites lie close to the direction of the Sun (at certain times of day), and for mobile satellite systems with large beamwidths and low signal-to-noise ratios [Franke, 1996].

8.9 GNSS – Total Electron Content (TEC) correction

Target risk: GNSS – Total Electron Content (TEC) correction	
Environmental risk parameter:	TEC and related gradients
Rationale:	The ionospheric range correction on GNSS position and time estimates is directly proportional to TEC, e.g. an uncorrected TEC value of 6×10^{16} m^{-2} gives a range correction of about 1m for the L1 GPS signal (1.575 GHz). This directly affects the performance of single point positioning systems (i.e. single frequency, single receiver) Some GNSS systems use augmentation systems (e.g. EGNOS), that measure TEC and send corrections to receivers. This assumes that TEC does not change significantly between the measurement and delivery of the correction. If the spatial or temporal rate of change of TEC is too large, the corrections will be inaccurate (as happened over the US during the October 2003 event). Precise point positioning (PPP) systems solve for the ionospheric error. However, large initial mis-modelling of the TEC, and poor uncertainty quantification, can increase the time to achieve convergence of the position solution.
Suggested worst case:	Defining a TEC of 1×10^{16} m^{-2} = 1TECu Midlatitude vertical TEC: 350 TECu based on model overbounding limits estimated by Schlüter and Hoque (2020). This is significantly greater than the largest measured value of 250 TECu on 30 October 2003 (Mannucci, 2010). Midlatitude TEC spatial range gradient: 800 mm km^{-1}, based on double the spatial gradient from Datta-Barua et al. (2010) for the same event. Midlatitude TEC temporal range gradient: 38 m min^{-1}, based on double the spatial gradient from Datta-Barua et al. (2010) and double the typical major storm time frontal velocities.
Worst case duration	Several days, but likely to be more severe on the first day when a positive storm event occurs. Note that positive storm events can occur on multiple days for multiple CME arrivals
Worst case spatial extent	Effects likely in regions all over the world. Further study needed to assess regional responses.
Anticipated effects	Inaccurate TEC corrections, leading to enhanced errors in GNSS position and timing.
Quality of case:	Effects have been clearly observed in GNSS systems.. Extrapolation of TEC for a worst case remains uncertain.

Target risk: GNSS – Total Electron Content (TEC) correction	
Provenance:	Vertical TEC: Schlüter and Hoque (2020), Mannucci (2010) TEC spatial range gradient: (Datta-Barua et al., 2010) TEC temporal range gradient (Datta-Barua et al., 2010) Duration: Expert assessment and past experience of ionospheric storm progression
How to improve case quality:	Real-time monitoring and modelling. Further evaluation of physics-based ionospheric models to run for extreme storm scenarios.
Other notes:	● Dual-, and triple-, frequency GNSS receivers allow TEC corrections without the need for augmentation or differential systems. These are common in geodesy, surveying, and are now found in many mobile phone GNSS devices. ● Vertical TEC values given – multiply by 2-3 to adjust for oblique paths and avoid using low-elevation satellites

8.10 GNSS – Effects of Ionospheric Scintillation

Target risk: GNSS – effects of Ionospheric Scintillation	
Environmental risk parameters:	Scintillation is caused by small scale irregularities which can be quantified by the strength of the turbulence parameter, CkL. Amplitude scintillation is often quantified by the S4 index. Phase scintillation is often quantified by the sigma-phi (σ_φ) index
Rationale:	Small-scale spatial irregularities in the ionosphere can diffract and refract radio signals. This causes rapid fluctuations in signal intensity and phase, known as amplitude and phase scintillation respectively. ● Amplitude scintillation can reduce radio signal intensity below a receiver's lock threshold, thereby causing loss of signal on GNSS and other satellite links). ● Phase scintillation may lead to cycle slips and loss of lock for receivers as they track the signal. Very intense scintillation is characterised by a Rayleigh amplitude distribution (and associated random phase) due to scattering of signals by multiple spatial irregularities.
Suggested worst case:	Rapid fluctuations in the amplitude and phase of radio signal, leading to errors in positioning of more than 100 m, and repeated losses of service, each lasting from seconds to tens of minutes.
Worst case duration	These effects will occur intermittently over a period lasting several days.
Worst case spatial extent	Large patches distributed across the globe. Storm induced ionospheric scintillation may occur at high and mid geomagnetic latitudes, and low latitude scintillation effects are also possible. CAVEAT: This scenario addresses the enhanced scintillation that arises during a geomagnetic storm. It does not address the diurnal ionospheric scintillation that occurs at equatorial latitudes, particularly when local time is in the evening hours.
Anticipated effects	Widespread degradation and potential loss of GNSS signals for location and timing – with economic impacts on the UK as studied by London Economics (2017).
Quality of case:	Studies by the international Satellite-based Augmentation Systems (SBAS) Ionospheric Working Group with representatives from the European, Japanese and US systems (EGNOS, MSAS and WAAS).

Target risk: GNSS – effects of Ionospheric Scintillation	
Provenance:	Peer-reviewed papers by Doherty (2000), Skone (2000), Ledvina et al (2002), Mitchell et al (2005) and Blanch et al (2012).
How to improve case quality:	● Better understanding of how intermittent reception of signals impacts GNSS applications, building on work by Ali (2017) (PhD: https://agupubs.onlinelibrary.wiley.com/doi/full/10.1029/2004GL021644) ● GNSS navigation and timing receivers have specific vulnerabilities that relate to the internal receiver configuration. Simulation testing of the effects of ionospheric scintillation on specific receiver configurations is necessary to understand the true impacts of space weather events (Pinto Jayawardena et al., 2017). .
Other notes:	Test equipment for GNSS scintillation has been developed through a Partnership at Spirent Communications/University of Bath.

8.11 Satcom - Effects of Ionospheric Scintillation

Target risk: Satcom - effects of Ionospheric Scintillation	
Environmental risk parameters:	Scintillation is caused by small scale irregularities which can be quantified by the strength of the turbulence parameter, CkL. Amplitude scintillation is often quantified by the S4 index. Phase scintillation often quantified by the σ_φ (sigma-phi) index
Rationale:	Small-scale spatial irregularities in the ionosphere can diffract and refract radio signals. This causes rapid fluctuations in signal intensity and phase, known as amplitude and phase scintillation respectively. ● Amplitude scintillation can reduce radio signal intensity below a receiver's lock threshold, thereby causing loss of signal on satellite links. ● Phase scintillation may lead to loss of lock for receivers as they track the signal. Both effects are significant at frequencies below 3 GHz. Very intense scintillation will be characterised by a Rayleigh amplitude distribution (and associated random phase) due to scattering of signals by multiple spatial irregularities.
Suggested worst case:	Rapid fluctuations in the amplitude and phase of radio signal, leading to repeated disruption of communications links.
Worst case duration	These effects will occur intermittently over a period lasting several days.
Worst case spatial extent	Global. Storm induced ionospheric scintillation covering all high and mid geomagnetic latitudes, and low latitude scintillation effects also possible. CAVEAT: This scenario addresses the enhanced scintillation that arises during a geomagnetic storm. It does not address the diurnal ionospheric scintillation that occurs at equatorial latitudes, particularly when local time is in the evening hours.
Anticipated effects	Potential loss of communications links for L-band, UHF and VHF systems that route signals via satellites.
Quality of case:	Tbd
Provenance:	Cannon et al (2013)
How to improve case quality:	● Calculation / simulation of simulation impacts on link budgets ● Understand when and how intermittent reception of signals impacts satcom applications

Target risk: Satcom - effects of Ionospheric Scintillation	
Other notes:	● L band and UHF satcom systems are potentially vulnerable but detailed impact will depend on a detailed engineering assessment against the reasonable worst-case conditions specified here. Such assessment is outside the scope of this document. ● AIS maritime reporting via VHF satcom (i.e. out of sight of land) is potentially vulnerable, but requires detailed engineering assessment, as above (and taking account of what may be low data rates). ● Satcom systems at frequencies above 3 GHz, such as C, X, Ku and Ka bands, do not suffer significant impacts from ionospheric scintillation.

8.12 Blackout of high frequency radio communications

Target risk: Blackout of high frequency radio communications	
Environmental risk parameters:	Absorption of high-frequency (3-30 MHz) radio waves in the upper atmosphere
Rationale:	Ionisation in the upper atmosphere at altitudes of 60 to 90 km ("D region") will absorb HF radio waves, so they cannot reach the higher ionospheric layers that can reflect these waves. In such "blackout" conditions, HF radio cannot be used for over-the-horizon radio communications.
Suggested worst case:	Total blackout of HF radio frequencies
Worst case duration	● Two or three hours during daytime at low- and mid-latitudes (when the absorption is caused by a large solar flare) ● Several days at high latitudes (when the absorption is caused by a strong solar energetic particle event – sometimes termed a polar cap absorption event)
Worst case spatial extent	● All low- and mid-latitude regions on the dayside of the Earth (when the absorption is caused by a large solar flare) ● High latitude regions (when the absorption is caused by a strong solar energetic particle event)
Anticipated effects	Loss of operation of HF radio systems
Quality of case:	Long-recognised issue with heritage back to 1930s (flare-induced effects) and the 1950s (SEP-induced effects).
Provenance:	Halcrow and Nisbet (1977), Jones and Stephenson (1975), Lockwood (1993), Rogers and Honary (2015), Rogers et al (2015), Schumer (2009), Sauer and Wilkinson (2008), Warrington et al (2012). Also, for commercial aviation operations: ICAO (2015).
How to improve case quality:	Increase international collaboration for collection of riometer measurements. Additional collaboration with airlines and ATC to identify operational and safety impacts that will validate improved ionospheric models for forecasting loss of HF.

Target risk: Blackout of high frequency radio communications	
Other notes:	In November 2019 a range of new 24/7 space weather services for aviation were launched by ICAO, These advisories focus on solar events that can potentially impact on air transport, including HF communications. These are delivered by three global consortia, with the Met Office a partner in the PECASUS consortium.. It has been suggested that the need for HF comms will disappear because of the use of line-of-sight datalink systems and satcom transmissions. Datalink does overcome some of the ATC difficulties for airspace management caused by disruption or loss of HF in the relevant regions, but in many emergency situations a voice call on HF is the quickest and safest option. The use of Satcom is not a viable tool for use by ATC to manage and control safe separations between multiple aircraft in normal or emergency situations (regardless of space weather activity). Therefore, it is considered that the use of HF will remain for at least the next 10-15 years.

8.13 Anomalous high frequency radio communications

NB This scenario will be expanded in future work by SEIEG, as indicated by several TBD entries. It is included here to indicate that work is planned.

Target risk: Anomalous high frequency radio communications	
Environmental risk parameters:	Anomalous propagation of high-frequency (3-30 MHz) radio waves in the upper atmosphere
Rationale:	At all latitudes severe storms can cause a significant reduction in the critical frequency of the F2-region, foF2, for periods of up to 3-days. At high and low latitudes additional reflecting structures, ionospheric gradients and irregularities occur. These manifest on HF paths as multipath causing frequency selective fading and Doppler distortion of HF signals.
Suggested worst case:	Mid-latitudes: Availability of frequencies reduces, especially during local night-time hours, and as a result of this the likelihood of interference increases. This extended reduction in foF2 may be preceded by a few hours of increased foF2 values in the early hours of the storm. Low and High-latitudes: 60 Hz Doppler spread, multipath spreads ranged 15 ms.
Worst case duration	● Mid-latitudes. TBD ● Low and High-latitudes: TBD
Worst case spatial extent	● Mid-latitudes. TBD ● Low and High-latitudes: TBD
Anticipated effects	Loss of operation of HF radio systems
Quality of case:	Long-recognised issue dating back to the early days of HF communications
Provenance:	Angling et al (1998) Cannon et al (2000)
How to improve case quality:	Evaluation of negative storm progression using the IRI storm model. Evaluation of negative storm progression using physics-based models to evaluate extreme events.
Other notes:	

8.14 Railway signal systems

Target risk: Railway signal systems	
Environmental risk parameter:	The geoelectric field, *E*, induced in the surface of the Earth by geomagnetic activity. In the UK, E-fields are particularly spatially complex, due to the underlying geology and surrounding seas .
Rationale:	Track circuits are widely used to detect the presence of trains on specific sections of railway track. The presence of the train changes the flow of electricity in the circuit, compared to an unoccupied track. If strong E-fields drive GIC into a track circuit, it may confuse the operation of that circuit. The response of DC track circuits to GIC has previously been modelled in detail by Boteler (2021) and provides clearer insights into the conditions under which DC track circuits can give incorrect information. This new modelling has been applied to a number of electrified UK rail routes by Patterson (2023a, 2023b , 2024a and 2024b).
Suggested worst case:	"Right side" failures are misoperations created when GICs cause the track circuit equipment to indicate a section of line is occupied by a train when it is not. "Wrong side" failures are misoperations that cause the track circuit equipment to indicate a line of section is empty by a train when it is actually occupied. "Wrong side" failures are clearly a hazardous case if a red signal preventing another train entering an occupied section is switched to green, causing the block to appear clear and giving no warning for approaching trains to stop. Modelling of the UK West Coast Main Line and the Glasgow to Edinburgh (via Falkirk) line by Patterson *et al.* (2024a) indicates that a 1-in-100 year or 1-in-200 year extreme storm would lead to multiple right- and wrong-side signalling failures.
Worst case duration	Strong geoelectric fields arise when the rate of change of the geomagnetic field (dB/dt) is large. The most intense dB/dt events are typically short bursts lasting a few minutes duration. Multiple bursts in d*B*/d*t* (a few minutes each) may be observed throughout an extreme geomagnetic storm lasting hours to days.
Worst case spatial extent	Growing evidence that these intense bursts (and the associated GIC events) have spatial scales of a few hundred km (Ngwira et al., 2015; Pulkkinen et al., 2015) and therefore could extend across the whole of the UK.

Target risk: Railway signal systems	
Anticipated effects	"Right-side failures" are disruptive as they can delay trains, but "wrong side failures" are dangerous as they can lead to train collisions. Recent work (Patterson, 2024a) has clarified the conditions under which the latter can occur. It requires not just a strong geoelectric field, but is most likely when a train is at the end of a track circuit block, i.e. furthest from the relay that controls the signal at the start of the block. Thus this is a risk linked to the affected system being in the "wrong place" at the "wrong time". Crucially, the impact of GICs on track circuits are non-destructive. Equipment misoperates, but is not otherwise damaged. Normal functionality should resume when the GICs subsides. However, this can be an obstacle to the reliable attribution of misoperations to space weather effects.
Quality of case:	Long-standing issue with reports dating back into the late 19th century, but has now gained renewed attention because of the global recognition that space weather is a natural hazard which can interfere with many engineered systems. This attention is driving new high-quality studies as noted elsewhere in this section.
Provenance:	Boteler (2021), Alm (2020), Lejdström & Svensson (2020), Patterson (2023a, 2023b , 2024a and 2024b).
How to improve case quality:	Need to extend existing studies of GIC impacts on UK rail systems (e.g. Patterson, 2023a, 2023b) to cover rail lines across the whole of the UK, e.g. as through the current UKRI/NERC-funded project "Modelling the impact of geomagnetically induced currents on UK railways" at Lancaster University. Studies of UK rail system anomalies have identified some events that were likely the consequence of space weather, notably some disruption in South Wales during the Halloween space weather event of 2003. However, the anomaly data is limited both in quality and quantity. It would be valuable to compile systemic databases of rail system anomalies and analyse those to better understand the level of impact during both moderate and severe space weather.

Target risk: Railway signal systems	
Other notes:	Track circuits were first introduced in the 1870s, and GIC interference with UK rail systems was observed during severe geomagnetic storms in the 1880s (Maunder, 1900). The impact of GIC on railway track circuits was the subject of a number of 1950s studies in Sweden as noted by Boteler (2021). Some of these have recently been made available in English (Alm; 2020; Lejdström & Svensson, 2020), and include methods for protection of circuits against "wrong-side failures" in which an occupied track section appears clear, thus creating a potential collision risk. More recent examples of space weather interference with track circuits has been reported in Sweden and Russia, e.g. see Eroshenko et al., 2010. Recent work in China has provided direct measurements of GIC in track circuits of modern high-speed lines (Liu et al., 2016).

8.15 Sub-orbital flight – avionics

Target risk: Sub-orbital flight – avionics	
Environmental risk parameter:	Solar energetic particles > 40 MeV
Rationale:	Solar energetic particles (e.g. protons) with energies above 40 MeV (and hence can cause single event effects) can penetrate Earth's atmosphere down to altitudes of 50 km or lower. Thus sub-orbital flights seeking to cross the von Karman line (100 km altitude) will be exposed to these particles, if geomagnetic shielding permits those particles to reach the geographic location of the flight. Thus the avionic systems in sub-orbital flights may be at risk of high SEE rates during SEP events, even if those events have soft spectra with low fluxes of the >400 MeV particles that generate high neutron fluxes at normal aircraft cruise altitudes.
Suggested worst case:	Worst case intensities same as for SEE effects on satellites, including allowance for geomagnetic cut-off, as discussed in detail in section 7.3.
Worst case duration	Worst case durations of several days, same as for SEE effects on satellites as discussed in section 7.3.
Worst case spatial extent	Considerable variations across the world due to the shielding effects of Earth's magnetosphere. Thus flights at high latitudes will be most vulnerable. This shielding will be reduced during strong magnetic storms, increasing the vulnerability of flights at mid-latitudes (such as from the UK).
Anticipated effects	High upset rates and possible high failure rates in inadequately protected digital avionic systems
Quality of case:	As with satellite SEE effects, this is based on extrapolation from space age measurements. This may be supplemented in future by use of cosmogenic isotopes to estimate historical SEP events; this is an area of ongoing research.
Provenance:	Dyer et al., 2004

Target risk: Sub-orbital flight – avionics	
How to improve case quality:	The NOAA Solar Radiation Storm S-scale, derived from the GOES >10 MeV solar proton energy channel, was designed for warning of harmful increases in solar radiation during NASA astronaut EVAs, and is likely to be useful here as lower energy protons will be an important factor for flights at high altitudes and high latitudes. But further work is needed to fully assess its application to sub-orbital flights. Data from monitors on board sub-orbital fights to stimulate development and validation of improved models of radiation exposure on such flights. Determination of susceptibility of avionics equipment and systems. Consider the susceptibility of new electronics to high-energy protons. The SWIMMR Aviation Risk Modelling (SWARM) has developed MAIRE+, a data-driven atmospheric radiation model to nowcast secondary particle fluxes, biological dose rates and electronic upset/failure rates throughout the atmosphere, including those from GLEs. Future developments will extend the atmospheric radiation model up to 100 km altitude, thus encompassing much of the flight environment for sub-orbital flights.
Other notes:	The short duration of sub-orbital flights, as currently being developed and executed, means that it will be challenging for operators to respond to nowcast warnings based on the S-scale for space radiation. That scale is dominated by lower energy particles (10s of MeV) that will arrive many minutes after the higher energy particles that are the main risk factor for sub-orbital flight. Thus if a radiation storm were to commence just before or during the early stages of a sub-orbital flight, any S-scale nowcast warning will arrive only later in the flight, possibly too late to adjust the flight trajectory. We note that a lack of preparation for incidents such as disruption of avionics by radiation storms could stymie growth of this industry sector. The history of UK aviation provides an example of how a poorly understood technical issue (metal fatigue in the first “Comet” passenger jets) acted to slow industry growth. (Higgs, 2018).

8.16 Aviation – avionics

Target risk: Aviation – avionics	
Environmental risk parameter:	Neutron fluence > 10 MeV
Rationale:	Secondary neutrons are the dominant source of single event effects below 60,000 feet. At altitudes above 60,000 feet ions make a significant contribution to SEEs and dose-equivalent for humans. The flux > 10 MeV is used in the standards but allowance must be made for lower energy neutrons, especially thermal, which can increase rates in certain components by a factor 10. Note that energetic protons can contribute significantly while for new technologies stopping protons and muons are increasingly significant.
Suggested worst case:	For a 1-in-150 year event, 4000-fold increase in radiation environment (2400-fold increase for 1-in-100 years), compared to solar minimum conditions, at 40,000 feet (12 km) and high latitude. This is based on a recent assessment of extreme events by Dyer et al. (2017). Using both the instrumental record and proxies such as ^{14}C and ^{10}Be, this assessment suggests to use a 1-in-150 year worst case 4 times more intense than the 23 Feb 1956 event, which is calculated to have produced a 1000-fold increase for high geomagnetic latitudes (Dyer et al., 2017). For the 1-in-150 year event at 40,000 feet neutron fluxes > 10 MeV are: ● $1.2x10^6$ $cm^{-2}hr^{-1}$ above London ● $2.3x10^7$ $cm^{-2}hr^{-1}$ above North of Scotland For the 1-in-100 year event at 40,000 feet neutron fluxes > 10 MeV are: ● $7.2x10^5$ $cm^{-2}hr^{-1}$ above London ● $1.4x10^7$ $cm^{-2}hr^{-1}$ above North of Scotland For higher latitudes there is essentially no geomagnetic shielding. For a 1 in 1000 year event, the distribution given in Dyer et al. (2017) suggests high latitude fluxes of 5 times worse than the above values for 1-in-150 years. For 1 in 10,000 years the factor increase is 12.5. For more detailed insights please see Tables 1 and 4 of Dyer et al. (2017). Fluxes are 3.6 times higher again at 60,000 feet (compared to 40000 feet) and high latitude. Above this altitude ions must also be considered.

Target risk: Aviation – avionics	
Worst case duration	Timescales of events range from 1 to 12 hours but note that for impulsive events such as Feb56, nearly all the fluence (77%) arrives in the first hour..
Worst case spatial extent	From the geomagnetic poles to about 45 degrees geomagnetic latitude. Effects may occur at lower latitudes if higher energy particles (>1 GeV) are present and penetrate to lower latitudes. If particles with energies up to around 15 or 16 GeV are present, the effects may reach the equator. Considerable regional variations across the world depending on the direction from which particles arrive, which varies with the direction of the interplanetary magnetic field. This can lead to marked differences between the northern and southern poles. If a ground level enhancement occurs during an extreme geomagnetic storm, then effects are more likely to be seen closer to the equator.
Anticipated effects	High upset rates and possible high failure rates in inadequately protected digital avionic systems
Quality of case:	This is based on observations of the ground level enhancement (GLE) radiation event of 23 Feb 1956 and comparison with other GLEs in the instrumental and proxy records, as consolidated by Dyer et al. (2017).
Provenance:	Peer-reviewed papers by Dyer et al (2003), Dyer et al (2007), Dyer et al. (2017), Lantos and Fuller (2003), Tylka and Dietrich (2009), Mekhaldi et al.(2015). 1956 observations in research note by Marsden et al (1956), Quenby and Webber (1959), Rishbeth, Shea and Smart (2009).

Target risk: Aviation – avionics	
How to improve case quality:	The NOAA Solar Radiation Storm S-scale, derived from the GOES >10 MeV solar proton energy channel, was designed for warning of harmful increases in solar radiation during NASA astronaut EVA's. It is now recognised that the vast majority of these protons are not sufficiently energetic to reach commercial airline cruising altitudes and will not give harmful radiation increases to flight crews and passengers. This is supported by flight radiation measurements carried out by SolarMetrics during several minor (S1-S3) radiation storms. Therefore the current S-scale is considered wholly inappropriate for use by airlines as an operational or duty of care decision-tool. Space weather events that produce significant solar proton fluxes with energies >400 MeV are required to yield increased flight doses and SEEs in avionics. More measurements on board aircraft, balloons, and by ground-based neutron monitors, to stimulate development and validation of improved models of radiation exposure. Further modelling of radiation in the upper atmosphere for UAVs, buoyant stratospheric balloons and space tourism. Determination of susceptibility of avionics equipment and systems. Consider susceptibility of new electronics to stopping protons and muons. The UK has developed the MAIRE+ real time model for atmospheric radiation. Also a set of SAIRA-A monitors are now flying routinely on commercial aircraft and SAIRA-B balloon monitors are available for launch into a GLE to calibrate the model. The MAIRE+ model will be transitioned to use the new UK ground level neutron monitors at Camborne and Lerwick as the main input data source in due course. Further studies to evaluate recent papers reporting on extreme radiation storms identified in proxy records such tree rings and ice cores. For example Bard et al (2023) have identified the strongest known cosmogenic SEP event in 14,300 BP (12,350 BCE) and Golubenko et al (2025) have calculated >200 MeV fluence of the 12,350 BCE event as 1.4×10^{10} cm^{-2}. This is 18% stronger than the 775CE/AD event.

Target risk: Aviation – avionics	
Other notes:	Assumes near worst case altitude (40,000 feet/12 km) and route (e.g. high latitude such as LHR-LAX or polar). Fluxes would be factor 3.6 worse at 60,000 feet and ions must be considered above this altitude. Any existing geomagnetic storm could expose lower latitude routes to similar fluxes. Effects are probably worst for short events that give high rates. Event durations are typically 1-12 hrs. Dyer et al. (2017) propose adoption of a new space weather scale for atmospheric radiation with February 1956 fluxes as the baseline for the scale. This would complement the NOAA S-scale for space radiation and would be far more appropriate for atmospheric radiation impacts. The use of this scale can be facilitated by the new UK ground level neutron monitors at Camborne and Lerwick.

8.17 Aviation – human radiation exposure

Target risk: Aviation – human radiation exposure	
Environmental risk parameter:	High radiation dose rates at aviation altitudes. Secondary neutrons are the main contribution below 60,000 feet but above this altitude ions make a significant contribution to SEEs and dose-equivalent for humans.
Rationale:	**Air crew**: are occupationally exposed. Airlines operate to a limit of 20 mSv per year and seek to keep doses below a constraint of 6 mSv per year. **Pregnant air crew:** airlines are expected to limit the dose received to 1 mSv, once they have been informed that their employee is pregnant. (In the US, the FAA guideline is 0.5 mSv in one month.) **Passengers including frequent business fliers**: not covered by legislation so no formal dose limits or constraints apply.
Suggested worst case:	**1 in 150 year event**: 28 mSv (17 mSv for 1 in 100 years), based on a recent assessment of extreme events by Dyer et al., 2017. Using both the instrumental record and proxies such as ^{14}C and ^{10}Be, this assessment suggests that the 1-in-150 year worst case would be 4 times more intense than the 23 Feb 1956 event, which is estimated to have produced a route ambient dose of 7 mSv at 40,000 ft on high latitude routes such as London to Los Angeles (Dyer et al., 2017). **1 in 1000 year event**: 150 mSv, based again on the assessment by Dyer et al., 2017, which takes account of extreme events in the proxy record, such as the 774 AD event (Miyake et al., 2012; Mekhaldi et al., 2015) For more details see Table 4 of Dyer et al. (2017)
Worst case duration	1-12 hours for a single event, but perhaps longer in a sustained series of events with several large X-class flares and fast CMEs. Note that for impulsive events such as Feb56, nearly all the dose (77%) arrives in the first hour.

Target risk: Aviation – human radiation exposure	
Worst case spatial extent	From the geomagnetic poles to about 45 degrees geomagnetic latitude. Effects may occur at lower latitudes if higher energy particles (>1 GeV) are present and penetrate to lower latitudes. If particles with energies up to around 15 or 16 GeV are present, the effects may reach the equator. Considerable regional variations across the world depending on the direction from which particles arrive, which varies with the direction of the interplanetary magnetic field. This can lead to marked differences between the northern and southern poles. If a ground level enhancement occurs during an extreme geomagnetic storm, then effects are more likely to be seen closer to the equator.
Anticipated effects	**Aircrew:** could exceed 6 mSv and airlines would seek to limit future doses by changes to flight duties. This may be logistically problematic. **Pregnant crew:** may exceed 1 mSv limit if they are still undertaking flight duties. However, airlines routinely change the flight duties of pregnant crew once they are notified of the pregnancy. **Passengers**: will need information on exposures received.
Quality of case:	This is based on observations of the ground level enhancement (GLE) radiation event of 23 Feb 1956 and comparison with other GLEs in the instrumental and proxy records, as consolidated by Dyer et al., 2017.
Provenance:	Papers by Dyer et al. (2007), Dyer et al. (2017), Lantos and Fuller (2003), and Tylka and Dietrich (2009). 1956 ground level observations in research note by Marsden et al (1956), Quenby and Webber (1959), Rishbeth, Shea and Smart (2009). 774 AD event: Miyake et al., (2012); Mekhaldi et al (2015).

Target risk: Aviation – human radiation exposure	
How to improve case quality:	The NOAA Solar Radiation Storm S scale, derived from the GOES >10MeV solar proton energy channel, is suitable warning for spacecraft, but not for aviation. A new warning indicator is required for aviation, based on particles that can reach aircraft altitudes. These may be based on ground-based neutron monitor data and/or satellite measurements of solar protons with energies >400MeV. More measurements on board aircraft and balloons, and by ground-based neutron monitors, to stimulate development and validation of improved models of radiation exposure. International agreement is needed to determine the thresholds for advising restrictions on take-off, and advice on rerouting or changing altitude. This should also be related to the susceptibility of avionics. The UK has developed the MAIRE+ real time model for atmospheric radiation. Also a set of SAIRA-A monitors are now flying routinely on commercial aircraft and SAIRA-B balloon monitors are available for launch into a GLE to calibrate the model. The MAIRE+ model will be transitioned to use the new UK ground level neutron monitors at Camborne and Lerwick as the main input data source in due course. These capabilities need to be combined into a coherent service. Further studies to evaluate recent papers reporting on extreme radiation storms identified in proxy records such tree rings and ice cores. For example, Bard et al (2023) have identified the strongest known cosmogenic SEP event in 14,300 BP (12,350 BCE) and Golubenko et al (2025) have calculated >200 MeV fluence of 12,350 BCE as 1.4 x10^{10} cm^{-2}. This is 18% stronger than the 775CE/AD event.

Target risk: Aviation – human radiation exposure	
Other notes:	Assumes near worst case altitude (12 km) and route (e.g. high latitude such as London-Los Angeles or polar). However, a simultaneous geomagnetic storm could produce similar doses for lower latitude routes. Doses are probably worst for short events that give high dose rates and little time for avoidance. Longer duration events could affect more flights and/or expose more passengers. Dyer et al. (2017) propose adoption of a new space weather scale for atmospheric radiation with February 1956 fluxes as the basepoint for the scale. The use of this scale could be facilitated by the new UK ground level neutron monitors at Camborne and Lerwick.

8.18 Public behaviour impacts

Target risk: Public behaviour impacts	
Risk parameter:	No consensus on quantitative parameters at this time, but keep under review.
Rationale:	Infrastructure failure following an extreme space weather event may result in behaviours such as public disorder or stockpiling that might be expected in a major crisis.
Suggested worst case:	Lack of public awareness/confidence combined with a very severe event (widespread power blackouts, major interruptions to GNSS-based services).
Worst case duration	Several days but possible long term effects in terms of decline in trust.
Worst case spatial extent	All of the UK. Similar problems in other affected countries.
Anticipated effects	We would usually anticipate pro-social, altruistic behaviour but worst case public behaviour events could be:- ● Rejection of scientific understanding in favour of conspiracy / rumour. This may become widespread on social media, counter-acting scientific advice. ● State actors may attempt to influence discourse through social media (for example, UK citizens were not sufficiently warned) or to attack infrastructure (cyber-attacks or sabotage attacks) ● Reframing of the event with negative consequences for social cohesion (for example, that Government is directing recovery efforts towards some groups more than others) ● Stockpiling (sometimes called 'panic buying'), becomes self-fulfilling prophecy as stocks run low. ● Millenarianism See Appendix 2 to this report for a detailed discussion
Quality of case:	This is based on evidence discussed in Appendix 2
Provenance:	McBeath (1999), House of Lords Science and Technology Committee (2005), Kerr (2011), Sciencewise (2014), Preston et al. (2015),
How to improve case quality:	Monitor developments in the research community
Other notes:	

1. 7.19 Transoceanic optical fibre cables

Target risk: Transoceanic optical fibre cables	
Environmental risk parameter:	Geoelectric field E integrated over the length of a transoceanic cable between external power supplies at onshore stations. This may be expressed quantitatively as a voltage.
Rationale:	Optical fibre cables have repeaters placed at intervals along their length. These boost the optical signal to ensure its transmission over the whole length of the cable. The repeaters are powered via an electric power line embedded in the cable; this line is powered from the onshore stations at both ends of the cable. Geomagnetic activity can induce significant voltage changes in the power line. The voltage applied at each onshore station is referenced to its local ground. Thus, when space weather creates an offset between these local grounds, that offset will increase or reduce the applied voltage (depending on the sign of the induced voltage). The size of the offset is determined by the geoelectric field integrated across the transoceanic path of the cable. The offset will drive GIC through the cable. This effect is well-known to the designers of transoceanic cables. They conventionally mitigate for the voltage offset by applying an Earth Potential Allowance (EPA) to the operating voltage across the cable. The EPA is their estimate of the maximum offset that may be induced by space weather. Thus the power supply is designed to operate robustly when an induced voltage with magnitude less than the EPA is added to, or subtracted from, the normal operating voltage. This robustness has been well-demonstrated by published reports of space weather impacts on transoceanic cable operations over the past seventy years. This includes impacts on both the co-axial cable systems that were widely introduced from the 1950s onwards (see report by Axe (1968)) and on the optical fibre cable systems introduced from the late 1980s onwards (see reports by Medford et al. (1989) and Lanzerotti et al. (1995, 2001). Both system types used repeaters to ensure signal propagation over the length of the cable. The concern today is whether new cables will use repeaters, based on modern electronics, that require less power (and lower current) and that this may lead

Target risk: Transoceanic optical fibre cables	
	to a reduction in operating voltages on transoceanic cables. This seems unlikely so long as reasonable values are used for the EPA, e.g. based on historical reports as in the present document. In this context, it is worth noting that the period from 2004 to 2023 saw no extreme geomagnetic storms, so current cable operators may have had little experience of dealing with severe storm effects. This long quiet spell was broken by the Gannon geomagnetic storm of May 2024.
Suggested worst case:	Integrated geoelectric field of 3000 volts across the length of the cable.
Worst case duration	Several minutes if the induced voltage arises from a large spike in dB/dt (the rate of change of the geomagnetic field) at one end of the cable. Observations show that the induced voltage will reverse during this time, exhibiting both large positive and negative values.
Worst case spatial extent	Large voltages may be induced in a cable if there is strong geomagnetic activity with a footprint anywhere along the length of the cable. Such footprints are commonly observed at UK latitudes during extreme geomagnetic storms. Thus most cables landing in the UK and elsewhere in north-west Europe could be impacted during an extreme event. Transatlantic cables to Iceland, Canada and beyond are particularly exposed because they remain at similar or higher geomagnetic latitudes over their whole length.
Anticipated effects	Damage to repeater systems on transoceanic cables, potentially requiring costly deep sea repairs.
Quality of case:	Based on published reports of impacts on transoceanic cable systems. These include impacts on both optical fibre cables, and on earlier co-axial cables (which used an equivalent system of repeaters supported by a power line embedded in the cable). Reported impacts on transatlantic optical fibre systems include induced voltages of 300 to 700 volts (Medford et al., 1989; Lanzerotti et al., 1995; Lanzerotti et al., 2001), whilst reported impacts on transatlantic co-axial systems include an extreme case in 1958 when the induced voltage reached at peak of 2650 volts before reversing sign to reach an opposite peak of 2100 volts just seven minutes later (Sanders, 1961). We take the larger value from the latter case as a guide for the worst case (rounding to 3000 volts)
Provenance:	Published reports as noted above, in particular the 1958 cable impact reported by Sanders (1961). Note that this geomagnetic storm (11 February 1958) was a very severe global event that caused a range of GIC

Target risk: Transoceanic optical fibre cables	
	impacts, including extensive damage to telephone and telegraph systems in Finland and Sweden (Nevanlinna et al, 2001; Karsberg et al, 1959). Boteler et al (2024) have recently developed a robust technique for modelling the voltage across the whole length of the cable - given knowledge of the cable design and route, the ocean depth and the conductivity of sea water and subsea lithosphere. This was verified against early impacts on transatlantic optical fibre systems as noted above. A recent study by a team from Google (Castellanos et al., 2022) provides some data on cable voltage fluctuations that arise during moderate geomagnetic activity, set along voltage fluctuations generated by ocean tides. It provides some helpful context, in particular the need to set this space weather risk analysis in context of the Earth Potential Allowance used in engineering design of the cable power systems.
How to improve case quality:	Look for further reports on voltages induced by space weather on transoceanic cables, especially from the modern era of optical fibre cables. Ideally these should be reports published in the technical literature so that the reports can be validated. Reports on voltages recorded during the 2024 Gannon storm would be a welcome addition to the knowledge base.
Other notes:	Transoceanic cables have been a backbone of global communications since the late 19th century: first for use by electric telegraph systems based on twisted copper wires, then for voice traffic carried over multiple channels in coaxial cables, and, since the late 1980s, for both voice and internet traffic using optical fibre technology. Today the undersea optical fibre cable network carries the vast bulk of transoceanic internet traffic. It is much preferred to conventional geosynchronous satcom links because of the inherent delay in sending radio signals to and from geosynchronous orbit. There is significant literature, especially from the coaxial cable era of the mid-20th century, about the scale of space weather impacts on these older systems and how those impacts were mitigated. As noted above, Sanders (1961) includes some detailed insights into the voltages induced a cable segment between Scotland and Newfoundland during a very severe geomagnetic storm on 11 February 1958. Another example is Axe (1968), which reports examples of large induced voltages observed on several subsea

Target risk: Transoceanic optical fibre cables	
	phone cables linking the UK to other countries, e.g. 600 volts on the link between Middlesbrough and Göteborg on 11 November 1960. It is important to recognise that the GICs that will flow in transoceanic cables are determined by the resistance of the power lines in those cables. These resistances are much higher than those in electricity transmission networks. Thus transoceanic cables will carry much lower levels of GICs than the tens or hundreds of amps observed to flow in electricity transmission networks during severe geomagnetic storms. Some analyses of GIC in these cables (e.g. Jyothi, 2021) have assumed that both cables and transmission networks will carry similar levels of GIC, and thus have significantly overstated the impact of space weather on transoceanic cables. Boteler et al. (2024) have carried out an in-depth analysis of the voltages induced in transoceanic cables.

9 Topics for future study

9.1 Electricity distribution networks

Most previous studies of space weather impacts on the transport of electrical power have focused on the transmission network that transports that power, often over long distances, from generators to the local distribution networks that deliver power to end users. The transmission network generally has lower line resistances with increasing voltage level (e.g. the Electricity Ten-Year Statement at Appendix B of https://www.neso.energy/publications/electricity-ten-year-statement-etys/etys-documents-and-appendices d), and hence will carry higher GIC in response to the geoelectric fields induced by space weather. Thus transmission subsystems, such as transformers, are more vulnerable to adverse effects of GIC, which increase as resistances decrease, and as further discussed in section 7.1.

However, it has been suggested (e.g. AbuHussein, 2018) that GIC could cause problems in the higher resistance distribution networks, and also to local power generation directly connected to those networks (e.g. some solar farms are connected to distribution networks). Further work is required to fully assess this risk and requires an engineering assessment of a range of technologies (e.g. the impact of GIC on inverters as discussed by AbuHussein (2018)), which is currently beyond the scope of future work for this document. For the purposes of this summary, we note that we will need to assess whether the worst case environment presented in section 7.1 is sufficient, or whether there will be a greater need to take account of local features (e.g. sharp lateral changes in subsurface conductivity, such as at the coast) that could amplify the geoelectric fields created by space weather.

9.2 Long-term change in the geomagnetic field

The internal geomagnetic field changes gradually over time, reflecting changes in the flow of the liquid iron in the Earth's core, which generates electric currents within the core, as the fluid advects across existing field lines (Roberts, 2015). This gradual change has important implications for space weather as the internal geomagnetic field structures many of the environments that we discuss in this document. For example, it determines the geographic location of the auroral zone, of the equatorial ionisation anomalies and of the South Atlantic Anomaly – regions where we frequently observe examples of intense geomagnetic activity, ionospheric scintillation and high-energy particle radiation respectively. Historical records suggest that the auroral zone has moved significantly over the centuries in response to changes in the geomagnetic field, whilst satellite observations over the past fifty years show that the SAA has moved slightly westwards towards South America, again in response to changes in the geomagnetic field.

We have good quantitative knowledge of how the geomagnetic field has evolved over recent centuries. This suggests, for example, that the 'wander' of the north geomagnetic pole, in latitude and longitude, has become more rapid in recent decades, moving from northern Canada in the direction of Siberia. At the same time, the southern pole has not shown the same characteristics. This has led to speculation that there could also be rapid changes in the geographic locations at which particular space weather environment exhibit severe conditions. Thus research into the future evolution of the geomagnetic field is important for assessing likely changes in the location and characteristics of those environments. Fortunately state-of-the-art modelling of the internal field as part of the UKRI/NERC funded SWIGS (Space Weather Impacts on Ground-based Systems) has recently done that, noting that "the space-weather related risk will not change significantly for the UK over the next 50 years" (Maffei et al., 2023).

Thus we conclude that the evolution of the internal field probably does not significantly affect the scenarios presented in this document, at least in the short term, and in so far as they directly affect the UK. But it is important to encourage and monitor future research to watch for any emerging issues that may directly affect the UK, and also to understand how the evolving field changes space weather environments elsewhere in the world.

9.3 Human spaceflight

Whilst preparing the current version of this summary, SEIEG members discussed whether additional risks from space weather should be considered in respect of human spaceflight, and how those risks might sit within the broader set of risks that space weather poses for the UK. By "additional risks" we mean risks that go beyond those that have already been identified as affecting robotic spacecraft. These risks, and the environments that drive them, are already discussed in detail in this summary (see sections 7.2 to 7.6 above), and apply equally to both robotic spacecraft and to spacecraft that carry a human crew. The only difference that we anticipate for these risks is that a higher standard of risk mitigation will apply to crewed spacecraft.

At present UK human spaceflight activities, e.g. flights to the ISS, are focused through the ESA astronaut programme, which is headquartered in Cologne and takes professional responsibility for the health and safety of all ESA astronauts. Thus the management of this risk is delegated to ESA and there appears to be no need for a separate UK assessment.

The need for a separate assessment could emerge in the future if UK human spacecraft activities were to develop as a national or commercial capability. Thus we outline some environmental characteristics that would then need to be considered:

1. The main additional risk for human spaceflight is radiation exposure of the human body (Cucinotta et al., 2013; Dietze et al., 2013). Space radiation (both cosmic rays from outside our solar system, and solar energetic particles produced by space weather events on the Sun) include particles at energies of 100s or 1000s of MeV that are likely to produce significant radiation levels inside a crewed spacecraft. The radiation exposure of astronauts will vary considerably depending on the trajectory and duration of the spaceflight. Sub orbital flights at low and mid latitudes will generally have the lowest exposure, as they will benefit from the screening of incoming radiation by the magnetosphere, and their short duration. Flights in low-Earth orbits (e.g. on the ISS) will also benefit from that magnetospheric screening, but will be much longer duration and will encounter the South Atlantic Anomaly (the region just south of Brazil where high fluxes of radiation belt particles reach LEO altitudes) for ten minute periods during some 8 of the 15 orbits per day (see, for example, Dyer et al. (2000) where typical time profiles are given from UK radiation monitors on the MIR Space Station which was in very similar orbit to the current ISS)). The daily dose is shared fairly evenly between GCRs and SAA protons. Exposure on the ISS has been studied widely, e.g. through use of space environment tools such as SPENVIS (Gustafsson et al., 2009), through dosimetry measurements on the ISS (Sihver et al.,. 2015; Spurný et al., 2007), through use of the Matroshka mannequin on the ISS to simulate the exposure experienced by a human body (Berger, 2013; Puchalska, 2012; Reitz et al, 2010), and through detailed Geant 4 modelling of the interior of the ISS (Ersmark, 2006; Ersmark et al., 2003, Ersmark et al., 2007a and 2007b). Radiation exposure will be greater for flights outside Earth's inner magnetosphere, e.g. to the surface of the Moon (Cucinotta et al., 2010; Zhang et al., 2020), or to the planned Lunar Gateway. The radiation exposure of astronauts will be significantly increased during SEP events, again with that exposure depending on the spacecraft trajectory. For extreme events the exposure levels would induce radiation sickness. The Apollo missions to the Moon are considered to have had a near-miss in this respect, when a very intense SEP event in August 1972 occurred between the flights of Apollo 16 and Apollo 17 (Lockwood and Hapgood, 2007).

2. Another potential risk is electrical charging of external surfaces as discussed in section 7.5. This could pose an additional risk to astronauts if electrical discharges occurred near astronauts when they work outside a spacecraft. Charging risks are generally modest in low Earth orbit, but are monitored in the case of ISS (Craven et al., 2009). In the future, charging may be a significant issue for missions to the Moon, as there is extensive evidence from Apollo and later missions for significant charging of the lunar surface (e.g. see discussion in Hapgood (2007)).

10 Glossary

AC	Alternating current
AE8	Model of electron fluxes in the radiation belts
AIS	Automatic Identification System, an automatic tracking system used by shipping.
ATC	Air traffic control
BAS	British Antarctic Survey
BCE	Before Christian Era
BGS	British Geological Survey
BP	Before Present (time)
CE/AD	Christian Era/Anno Domini
CHAMP	Challenging Minisatellite Payload (DLR satellite)
CME	Coronal mass ejection
DC	Direct current
DSTL	Defence Science and Technology Laboratory
EGNOS	European Geostationary Navigation Overlay Service (European SBAS)
EPA	Earth Potential Allowance
EUV	Extreme ultra-violet
EVA	Extra vehicular activity
FAA	Federal Aviation Administration
GCR	Galactic cosmic ray
GB	Great Britain (England, Scotland and Wales)
GEO	Geosynchronous orbit
GIC	Geomagnetically induced currents
GLE	Ground Level Enhancement
GNSS	Global Navigation Satellite System
GOES	Geostationary Operational Environmental Satellite
GRACE	Gravity Recovery and Climate Experiment. Joint NASA/DLR satellite.
HF	High Frequency (3 to 30 MHz) radio
ICAO	International Civil Aviation Organisation
keV	Kilo-electron-volt
L-band	Radio frequencies between 1 and 2 GHz
LAX	Los Angeles international airport
LEO	Low Earth Orbit
LHR	London Heathrow airport
MEO	Medium Earth Orbit
MeV	mega electron-volt
MSAS	Multi-functional Satellite Augmentation System (Japanese SBAS)
mSv	millisievert – unit of radiation dose for human exposure (effective dose or dose equivalent).
NERC	Natural Environment Research Council
NESO	National Energy System Operator
NOAA	National Oceanic and Atmospheric Administration
PECASUS	Pan-European Consortium for Aviation Space weather User Services
SAA	South Atlantic Anomaly

SAGE	SWIMMR Activities in Ground Effects
SAPPHIRE	Solar Accumulated and Peak Proton and Heavy Ion Radiation Environment model
SBAS	Satellite-based Augmentation System (for GNSS)
SCATHA	US Air Force satellite mission to study charging effects, flown in late 1970s and early 1980s.
SEE	Single event effect
SEP	Solar energetic particle
SFU	Solar flux unit (measure of solar radio signal strength); 1 SFU = 10^{-22} $Wm^{-2}Hz^{-1}$)
SRB	Solar radio burst
SPEN	SP Energy Networks
SWIGS	Space Weather Impact on Ground-based Systems
SWIMMR	Space Weather Instrumentation, Measurement, Modelling and Risk (research programme)
TBD	To be done
UAV	Unmanned Aerial Vehicle
UHF	Ultra High Frequency (300 MHz to 3 GHz) radio
VHR	Very High Frequency (30 to 300 MHz) radio
WAAS	Wide Area Augmentation System (US SBAS)
UKSA	UK Space Agency
UKRI	UK Research and Innovation

11 References

AbuHussein, A. (2018). Impact of Geomagnetically Induced Current on Distributed Generators. In 2018 IEEE/PES Transmission and Distribution Conference and Exposition (T&D) (pp. 1-5). IEEE. https://doi.org/10.1109/TDC.2018.8440381

Alm, E. (2020). Measures against geomagnetic disturbances in the entire DC track circuit for automatic signalling systems. Infrastructure Resilience Risk Reporter, 1(10), 10–27. https://carleton.ca/irrg/journal/. (English translation of Alm, E. (1956). Åtgärder mot jordmagnetiska störningar i Hela Likströmsspårledningar föe automatiska vägsignalanläggningar, Bilaga 5F, Betänkande: Angående det tekniska utförandet av signalanläggningar vid Statens Järnvägar.)

Angling, M. J., Cannon, P.S., Davies, N.C., Willink, T.J., Jodalen, V. and Lundborg, B. (1998). Measurements of Doppler and Multipath Spread on Oblique High-Latitude HF Paths and their use in Characterising Data Modem Performance, Radio Sci., 33, 97-107, doi: 10.1029/97RS02206

Axe, G. (1968) The Effects of the Earth's Magnetism on Submarine Cables. Post Office Electrical Engineers' Journal. 37-43.

Bard Edouard, Miramont Cécile, Capano Manuela, Guibal Frédéric, Marschal Christian, Rostek Frauke, Tuna Thibaut, Fagault Yoann and Heaton Timothy J. (2023) A radiocarbon spike at 14 300 cal yr BP in subfossil trees provides the impulse response function of the global carbon cycle during the Late Glacial, *Phil. Trans. R. Soc. A*. 381: 20220206, https://doi.org/10.1098/rsta.2022.0206

Beggan, C. D., D. Beamish, A. Richards, G. S. Kelly, and A. W. P. Thomson (2013), Prediction of extreme geomagnetically induced currents in the UK high-voltage network, *Space Weather* 11, 407–419, doi:10.1002/swe.20065.

Berger, T., Bilski, P., Hajek, M., Puchalska, M. & Reitz, G. (2013) The Matroshka Experiment: Results and comparison from extravehicular activity (MTR-1) and intravehicular activity (MTR-2a/2b) exposure. *Radiation Research*, 180, 622-637.

Berger, T. E., Holzinger, M. J., Sutton, E. K., & Thayer, J. P. (2020). Flying through uncertainty. *Space Weathe*r, 18, e2019SW002373. doi: 10.1029/2019SW002373

Berger, T. E., Dominique, M., Lucas, G., Pilinski, M., Ray, V., Sewell, R., et al. (2023). The thermosphere is a drag: The 2022 Starlink incident and the threat of geomagnetic storms to low earth orbit space operations. *Space Weather*, 21, e2022SW003330. https://doi.org/10.1029/2022SW003330

Blake, S. P., Gallagher, P. T., McCauley, J., Jones, A. G., Hogg, C., Campanyà, J.,…Bell, D. (2016). Geomagnetically induced currents in the Irish power network during geomagnetic storms. *Space Weather*, 14, 1–19. doi: 10.1002/2016SW001534

Blake, S. P., Gallagher, P. T., Campanyà, J., Hogg, C., Beggan, C. D., Thomson, A. W. P., et al. (2018). A detailed model of the Irish high voltage power network for simulating GICs. Space Weather, 16, 1770– 1783. Doi: 10.1029/2018SW001926

Blanch, J., Walter, T., & Enge, P. (2012). Satellite navigation for aviation in 2025. Proceedings of the IEEE, 100(Special Centennial Issue), 1821-1830. https://doi.org/10.1109/JPROC.2012.2190154

Boteler, D. H. (2019). A 21st century view of the March 1989 magnetic storm. Space Weather, 17, 1427– 1441. Doi: 10.1029/2019SW002278

Boteler, D. H. (2021). Modeling geomagnetic interference on railway signaling track circuits. Space Weather, 19, e2020SW002609. Doi: 10.1029/2020SW002609

Boteler, D. H., Chakraborty, S., Shi, X., Hartinger, M. D., & Wang, X. (2024). An examination of geomagnetic induction in submarine cables. Space Weather, 22, e2023SW003687. https://doi.org/10.1029/2023SW003687

Brehm, N., Christl, M., Adolphi, F., Muscheler, R., Synal, H. A., Mekhaldi, F., ... & Wacker, L. (2021). Tree rings reveal two strong solar proton events in 7176 and 5259 BCE. Under review. Preprint on https://doi.org/10.21203/rs.3.rs-753272/v1
Bruinsma, S., de Wit, T. D., Fuller-Rowell, T., Garcia-Sage, K., Mehta, P., Schiemenz, F., ... & Elvidge, S. (2023). Thermosphere and satellite drag. Advances in Space Research https://doi.org/10.1016/j.asr.2023.05.011
Cabinet Office (2017) National Risk Register of Civil Emergencies – 2017 Edition https://www.gov.uk/government/publications/national-risk-register-of-civil-emergencies-2017-edition
Cagniard, L. (1953) Basic theory of the magneto-telluric method of geophysical prospecting, *Geophysics* 18, 605–635
Cannon, P. S., Angling, M.J., Clutterbuck, C., and Dickel, G. (2000). Measurements of the HF Channel Scattering Function Over Thailand, paper presented at Millenium Conference on Antennas and Propagation (AP2000), Davos, Switzerland. Pub. ESA, Publications Division, c/o ESTEC, PO Box 299, 2200 AG Noordwijik, The Netherlands.
Cannon, P., Angling, M., Barclay, L., Curry, C., Dyer, C., Edwards, R., Greene, G., Hapgood, M., Horne, R. B., Jackson, D., Mitchell, C., Owen, J., Richards, A., Rogers, C., Ryden, K., Saunders, S., Sweeting, M., Tanner, R. & Thomson, A. (2013). Extreme space weather: impacts on engineered systems and infrastructure. Royal Academy of Engineering. https://www.raeng.org.uk/publications/reports/space-weather-full-report
Castellanos, J. C., Conroy, J., Kamalov, V., Cantono, M., & Hölzle, U. (2022). Solar storms and submarine internet cables. arXiv preprint arXiv:2211.07850. https://doi.org/10.48550/arXiv.2211.07850
Cerruti, A.P., Kintner, P.M., Gary, D.E., Mannucci, A.J, Meyer, R.F, Doherty, P., and Coster, A.J. (2008) Effect of intense December 2006 solar radio bursts on GPS receivers. *Space Weather* 6, S10D07, doi:10.1029/2007SW000375.
Cid, C., Guerrero, A., Saiz, E., Halford, A. J., & Kellerman, A. C. (2020). Developing the LDi and LCi geomagnetic indices, an example of application of the AULs framework. Space Weather, 18, e2019SW002171. Doi: 10.1029/2019SW002171
Clilverd, M. A., Rodger, C. J., Brundell, J. B., Dalzell, M., Martin, I., Mac Manus, D. H., et al. (2018). Long-lasting geomagnetically induced currents and harmonic distortion observed in New Zealand during the 7–8 September 2017 disturbed period. Space Weather, 16, 704– 717. Doi: 10.1029/2018SW001822
Cliver, E.W. and Dietrich, W.F. (2013) The 1859 space weather event revisited: limits of extreme activity, *J. Space Weather Space Clim.* 3, A31, doi: 10.1051/swsc/2013053
Craven, P., Wright, K., Minow, J., Coffey, V., Schneider, T., Vaughn, J., ... & Parker, L. (2009). Survey of international space station charging events. In 47th AIAA Aerospace Sciences Meeting Including the New Horizons Forum and Aerospace Exposition (p. 119). https://doi.org/10.2514/6.2009-119
Cucinotta, F. A., Hu, S., Schwadron, N. A., Kozarev, K., Townsend, L. W., and Kim, M.-H. Y. (2010), Space radiation risk limits and Earth-Moon-Mars environmental models, Space Weather, 8, S00E09, doi:10.1029/2010SW000572.
Cucinotta, F. A., Kim, M. Y., & Chappell, L. J. (2013). Space radiation cancer risk projections and uncertainties-2012. NASA/TP-2013-217375. https://ntrs.nasa.gov/api/citations/20130001648/downloads/20130001648.pdf
Dietze, G., Bartlett, D. T., Cool, D. A., Cucinotta, F. A., Jia, X., Mcaulay, I. R., Pelliccioni, M., Petrov, V., Reitz, G. & Sato, T. (2013) ICRP, 123. Assessment of radiation exposure of astronauts in space. ICRP Publication 123. Ann ICRP, 42, 1-339.

Divett, T., Ingham, M., Beggan, C. D., Richardson, G. S., Rodger, C. J., Thomson, A. W. P., & Dalzell, M. (2017). Modeling geoelectric fields and geomagnetically induced currents around New Zealand to explore GIC in the South Island's electrical transmission network. *Space Weather*, 15, 1396–1412. doi: 10.1002/2017SW001697
Doherty, P. (2000) Ionospheric Scintillation Effects in Equatorial and Auroral Regions, ION GPS 2000, Salt Lake City, Utah, p. 662-671.
Datta-Barua, S., Lee, J., Pullen, S., Luo, M., Ene, A., Qiu, D., ... & Enge, P. (2010). Ionospheric threat parameterization for local area global-positioning-system-based aircraft landing systems. Journal of Aircraft, 47(4), 1141-1151. Doi: 10.2514/1.46719
Dyer, C. S., Truscott, P. R., Sanderson, C., Watson, C., Peerless, C. L., Knight, P., Mugford, R., Cousins, T. and Noulty, R. (2000) Radiation Environment Measurements from CREAM and CREDO During the Approach to Solar Maximum. IEEE Transactions on Nuclear Science, 47, 2208-2217. Doi: 10.1109/23.903755
Dyer, C. S., Lei, F., Clucas, S. N., Smart, D.F., Shea, M. A. (2003) "Solar particle enhancements of single event effect rates at aircraft altitudes," *IEEE Trans. Nuc. Sci.* 50, 2038-2045. doi: 10.1109/TNS.2003.821375
Dyer C.S., Hunter, K., Clucas, S., Campbell, A., (2004) " Observation of the solar particle events of October & November 2003 from CREDO and MPTB," *IEEE Trans. Nuc. Sci.* 51, 3388-3393. doi: 10.1109/TNS.2004.839156
Dyer, C.S., Lei, F., Hands, A., Truscott, P. (2007) "Solar Particle Events In The QinetiQ Atmospheric Radiation Model, " *IEEE Trans. Nuc. Sci.* 54, 1071-1075.
Dyer, C., A. Hands, K. Ryden and F. Lei, (2017) Extreme Atmospheric Radiation Environments & Single Event Effects, IEEE Trans. Nucl. Sci. doi: 10.1109/TNS.2017.2761258
Dyer, A., A. Hands, K. Ryden,C Dyer, I. Flintoff, and A.Ruffenach, (2020) Single Event Effects in Ground Level Infrastructure During Extreme Ground Level Enhancements, , IEEE Trans. on Nucl. Sci.. doi: 10.1109/TNS.2020.2975838
Eastwood, J. P., E. Biffis, M. A. Hapgood, L. Green, M. M. Bisi, R. D. Bentley, R. Wicks, L.-A. McKinnell, M. Gibbs, and C. Burnett (2017), The economic impact of space weather: where do we stand?, *Risk Analysis*, 37, 206-218. https://dx.doi.org/10.1111/risa.12765.
Eastwood, J. P., Hapgood, M. A., Biffis, E., Benedetti, D., Bisi, M. M., Green, L., et al. (2018). Quantifying the economic value of space weather forecasting for power grids: An exploratory study. *Space Weather*, 16. https://doi.org/10.1029/2018SW002003
ECSS-E-ST-10-04C Rev.1: European Cooperation for Space Standardization, (2020), Space environment, . https://ecss.nl/standard/ecss-e-st-10-04c-rev-1-space-environment-15-june-2020/.
EirGrid (2021) The Grid. https://www.eirgridgroup.com/the-grid/ (last accessed 5 Dec 2021)
Ersmark, T. (2006). Geant4 Monte Carlo Simulations of the International Space Station Radiation Environment (PhD dissertation, KTH). Retrieved from http://urn.kb.se/resolve?urn=urn:nbn:se:kth:diva-4007
Ersmark, T., Carlson, P., Daly, E., Fuglesang, C., Gudowska, I., Lund-Jensen, B., Nartallo, R., Nieminen, P., Pearce, M., Santin, G. & Sobolevsky, N. (2003) Status of the DESIRE project: Geant4 physics validation studies and first results from Columbus/ISS radiation simulations. 2003 IEEE Nuclear Science Symposium. Conference Record (IEEE Cat. No.03CH37515), pp. 1540-1544 Vol.3. Doi: 10.1109/NSSMIC.2003.1352170
Ersmark, T., Carlson, P., Daly, E., Fuglesang, C., Gudowska, I., Lund-Jensen, B., Nieminen, P., Pearce, M. & Santin, G. (2007a) Geant4 Monte Carlo Simulations of the Belt Proton Radiation Environment On Board the International Space Station/Columbus. IEEE Transactions on Nuclear Science, 54, 1444-1453.

Ersmark, T., Carlson, P., Daly, E., Fuglesang, C., Gudowska, I., Lund-Jensen, B., Nieminen, P., Pearce, M. & Santin, G. (2007b) Influence of geometry model approximations on Geant4 simulation results of the Columbus/ISS radiation environment. Radiation Measurements, 42, 1342-1350.
Erinmez, I. A., J. G. Kappenman, and W. A. Radasky (2002), Management of the geomagnetically induced current risks on the national grid company's electric power transmission system., *Journal of Atmospheric and Solar-Terrestrial Physics* 64, 5-6, 743-756. doi: 10.1016/S1364-6826(02)00036-6
Eroshenko, E.A., A.V. Belov, D. Boteler, S.P. Gaidash, S.L. Lobkov, R. Pirjola, L. Trichtchenko (2010) Effects of strong geomagnetic storms on Northern railways in Russia, *Adv. Space Res.* 46, 1102-1110. doi: 10.1016/j.asr.2010.05.017
Fennell, J. F. ; Koons, H. C. ; Roeder, J. L. ; Blake, J. B. (2001) Spacecraft Charging: Observations and Relationship to Satellite Anomalies, Aerospace Report TR-2001(8570)-5 http://www.dtic.mil/cgi-bin/GetTRDoc?AD=ADA394826
Gaunt C.T: (2014) Reducing uncertainty – responses for electricity utilities to severe solar storms. *J. Space Weather Space Clim.* 4, A01. doi: 10.1051/swsc/2013058
Golubenko, K., Usoskin, I. , Rozanov, E. & Bard, E. New SOCOL:14C-Ex model reveals that the Late-Glacial radiocarbon spike in 12350 BC was caused by the record-strong extreme solar storm (2025), Earth and Planetary Science Letters, 661, 119383, https://doi.org/10.1016/j.epsl.2025.119383.
Gustafsson, K., Sihver, L., Mancusi, D., Sato, T. & Niita, K. (2009) Simulations of the radiation environment at ISS altitudes. Acta Astronautica, 65, 279-288. Doi: 10.1016/j.actaastro.2009.01.040
Halcrow, B. W., and J. S. Nisbet (1977), A model of F2 peak electron densities in the main trough region of the ionosphere, Radio Sci., **12**(5), 815–820, Doi:10.1029/RS012i005p00815.
Feynman, J., G. Spitale, J. Wang, and S. Gabriel (1993), Interplanetary proton fluence model: JPL 1991, *J. Geophys. Res.* 98, 13,281–13,294, doi:10.1029/92JA02670.
Franke, E. (1996). Effects of solar, Galactic and man-made noise on UHF SATCOM operation. In Proceedings of MILCOM'96 IEEE Military Communications Conference (Vol. 1, pp. 29-36). IEEE. Doi: 10.1109/MILCOM.1996.568578
Ginet, G. P., O'Brien, T. P., Huston, S. L., Johnston, W. R., Guild, T. B., Friedel, R., ... & Madden, D. (2013). AE9, AP9 and SPM: New models for specifying the trapped energetic particle and space plasma environment. Space science reviews, 179, 579-615, doi: 10.1007/s11214-013-9964-y
Halford, A. J., Kellerman, A. C., Garcia-Sage, K., Klenzing, J., Carter, B. A., McGranaghan, R. M., Guild, T., Cid, C., Henney, C. J., Yu Ganushkina, N., Burrell, A. G., Terkildsen, M., Welling, D. T., Murray, S. A., Leka, K. D., McCollough, J. P., Thompson, B. J., Pulkkinen, A., Fung, S. F., Bingham, S., Bisi, M. M., Liemohn, M. W., Walsh, B. M., & Morley, S. K. (2019). Application Usability Levels: A framework for tracking project product progress. Space Weather and Space Climate, 9, 27. https://doi.org/10.1051/swsc/2019030
Hands, A. D. P., Ryden, K. A., Meredith, N. P., Glauert, S. A., & Horne, R. B. (2018). Radiation effects on satellites during extreme space weather events. Space Weather, 16, 1216–1226. https://doi.org/10.1029/2018SW001913
Hapgood, M. (2007) Modelling long-term trends in lunar exposure to the Earth's plasmasheet, Ann. Geophys., 25, 2037–2044, https://doi.org/10.5194/angeo-25-2037-2007
Hapgood, M., Liu, H., & Lugaz, N. (2022). SpaceX—Sailing close to the space weather? Space Weather, 20, e2022SW003074. https://doi.org/10.1029/2022SW003074
Hey, J.S. (1946) Solar Radiations in the 4–6 Metre Radio Wave-Length Band. Nature 157:47-48. doi:10.1038/157047b0

Higgs, C. (2018) De Havilland Comet: The World's First Commercial Jetliner. Pen and Sword Books, Barnsley, UK. ISBN-13 : 978-1526719614
House of Lords Science and Technology Committee (2005) *Pandemic Influenza: Report with Evidence*, HMSO: London, 124. https://publications.parliament.uk/pa/ld200506/ldselect/ldsctech/88/88.pdf
HSE (Health and Safety Executive). (1992). The tolerability of risk from nuclear power stations. http://www.onr.org.uk/documents/tolerability.pdf (Last accessed 29 Nov 2021)
Horne, R. B., Lam, P. Y., Meredith, N. P., Glauert, S. A., & Kirsch, P. (2025). Satellite internal charging for a reasonable worst-case. Space Weather, 23, e2024SW004226. https://doi.org/10.1029/2024SW004226
Hübert, J., Eaton, E., Beggan, C. D., Montiel-Álvarez, A. M., Kiyan, D., & Hogg, C. (2025). Developing a new ground electric field model for geomagnetically induced currents in Britain based on long-period magnetotelluric data. *Space Weather*, 23, e2025SW004427. https://doi.org/10.1029/2025SW004427
ICAO (2015), North Atlantic Operations and Airspace Manual.
Jackson, D. R., Fuller-Rowell, T. J., Griffin, D. J., Griffith, M. J., Kelly, C. W., Marsh, D. R., & Walach, M.-T. (2019). Future directions for whole atmosphere modeling: Developments in the context of space weather. Space Weather, 17, 1342– 1350. doi: 10.1029/2019SW002267
Jiggens, P. et al., (2018) The Solar Accumulated and Peak Proton and Heavy Ion Radiation Environment (SAPPHIRE) Model, *IEEE Trans. Nucl. Sci*, doi: 10.1109/TNS.2017.2786581
Jones, R. M., and J. J. Stephenson (1975), A versatile three-dimensional ray-tracing computer program for radio waves in the ionosphere, Rep. OT 75–76, Off. for Telecommun., U.S. Dep. of Comm., Washington, D. C.
Jyothi, S. A. (2021) Solar superstorms: planning for an internet apocalypse. In Proceedings of the 2021 ACM SIGCOMM 2021 Conference (pp. 692-704).
Kappenman, J.G. (2006) Great geomagnetic storms and extreme impulsive geomagnetic field disturbance events – An analysis of observational evidence including the great storm of May 1921, *Adv. Space Res*. 38, 188-199. doi: 10.1016/j.asr.2005.08.055
Karsberg, A. et al. (1959). The influences of earth magnetic currents on telecommunication lines. Tele (English ed.), Televerket, Stockholm, 1-21.
Kelly, G. S., A. Viljanen, C. D. Beggan, and A. W. P. Thomson (2017), Understanding GIC in the UK and French high-voltage transmission systems during severe magnetic storms, *Space Weather*, 15, 99–114, doi:10.1002/2016SW001469.
Kerr, R. (2011) Into the Stretch for Science's Point Man on Doomsday, Science, 6045, 333, 929-929. DOI: 10.1126/science.333.6045.928
Koons, H. C. (2001), Statistical analysis of extreme values in space science, *J. Geophys. Res.*, 106(A6), 10,915–10,921, doi:10.1029/2000JA000234.
Krausmann, E., Andersson, E., Russell, T., Murtagh, W. (2015): JRC report: Space Weather and Rail: Findings and Outlook. doi:10.2788/211456
Krauss, S., M. Temmer, A. Veronig, O. Baur, and H. Lammer (2015), Thermospheric and geomagnetic responses to interplanetary coronal mass ejections observed by ACE and GRACE: Statistical results, *J. Geophys. Res*.120, 8848–8860, doi:10.1002/2015JA021702.
Krauss, S., Temmer, M., & Vennerstrom, S. (2018). Multiple satellite analysis of the Earth's thermosphere and interplanetary magnetic field variations due to ICME/CIR events during 2003–2015. Journal of Geophysical Research: Space Physics, 123, 8884–8894. https://doi.org/10.1029/2018JA025778
Lantos, P., Fuller, N. (2003) "History of the solar particle event radiation doses on-board aeroplanes using a semi-empirical model and Concorde measurements," *Radiation Protection Dosimetry* 104, 3, 199-210.

Lanzerotti, L.J., Medford, L.V., Maclennan, C.G. and Thomson, D.J. (1995), Studies of Large-Scale Earth Potentials Across Oceanic Distances. AT&T Technical Journal, 74: 73-84. Doi: 10.1002/j.1538-7305.1995.tb00185.x
Lanzerotti, L. J., L. V. Medford, C. G. Maclennan, J. S. Kraus, J. Kappenman, and W. Radasky (2001), Trans-Atlantic geopotentials during the July 2000 solar event and geomagnetic storm, Solar Physics, 204, 351-359, doi: 10.1023/A:1014289410205.
Lawrence, E., Beggan, C. D., Richardson, G. S., Reay, S., Thompson, V., Clarke, E., ... & Smedley, A. D. (2025). The geomagnetic and geoelectric response to the May 2024 geomagnetic storm in the United Kingdom. Frontiers in Astronomy and Space Sciences, 12, 1550923. https://doi.org/10.3389/fspas.2025.1550923
Le, H., Liu, L., Ren, Z., Chen, Y., Zhang, H., and Wan, W. (2016), A modeling study of global ionospheric and thermospheric responses to extreme solar flare, J. Geophys. Res. Space Physics, 121, 832– 840, doi:10.1002/2015JA021930.
Lejdström, B., & Svensson, S. (2020). Calculation of geomagnetic interference voltages in track circuits (Translation into English of Lejdström and Svensson (1956)). Infrastructure Resilience Risk Reporter, 1(10), 28–51. June 2020. https://carleton.ca/irrg/journal/ (English translation of Lejdström, B. & Svensson, S. (1956). Beräkning av jordmagnetiska störningsspänningar i spårledningar, Bilag 6, Betänkande: angående det tekniska utförandet av signalanläggningar vid Statens Järnvägar.)
Ledvina, B. M., J. J. Makela, and P. M. Kintner, First observations of intense GPS L1 amplitude scintillations at midlatitude, Geophys. Res. Lett., 29(14), doi:10.1029/2002GL014770, 2002.
Liu, H., and H. Lühr (2005), Strong disturbance of the upper thermospheric density due to magnetic storms: CHAMP observations, *J. Geophys. Res.*, 110, A09S29, doi:10.1029/2004JA010908.
Liu, L. et al. (2016). Analysis of the monitoring data of geomagnetic storm interference in the electrification system of a high-speed railway. Space Weather 14, 754–763. doi:10.1002/2016SW001411.
Lockwood, M. (1993), Modelling the high latitude ionosphere for time varying plasma convection. *Proceedings of the IEE*, part H, *140(2)*, 91-100.
Lockwood, M., & Hapgood, M. (2007). The rough guide to the Moon and Mars. Astronomy & Geophysics, 48(6), 6-11. https://doi.org/10.1111/j.1468-4004.2007.48611.x
London Economics, 2017. The economic impact on the UK of a disruption to GNSS, http://tinyurl.com/yd9a5fhq
Love, J. J. (2012), Credible occurrence probabilities for extreme geophysical events: Earthquakes, volcanic eruptions, magnetic storms, *Geophys. Res. Lett.* 39, L10301, doi:10.1029/2012GL051431.
Mac Manus, D. H., Rodger, C. J., Dalzell, M., Thomson, A. W. P., Clarke, E., & Clilverd, M. A. (2017). Long term geomagnetically induced current observations from New Zealand: Earth return corrections and comparison with geomagnetic field driver. *Space Weather,* 15, 1020–1038. doi: 10.1002/2017SW001635
Mac Manus, D. H., Rodger, C. J., Ingham, M., Clilverd, M. A., Dalzell, M., Divett, T., et al. (2022). Geomagnetically induced current model in New Zealand across multiple disturbances: Validation and extension to non-monitored transformers. *Space Weather*, 20, e2021SW002955. https://doi.org/10.1029/2021SW002955
Mac Manus, D. H., Rodger, C. J., Renton, A., Ronald, J., Harper, D., Taylor, C., et al. (2023). Geomagnetically induced current mitigation in New Zealand: Operational mitigation method development with industry input. *Space Weather*, 21, e2023SW003533. https://doi.org/10.1029/2023SW003533

Maffei, S., Eggington, J. W., Livermore, P. W., Mound, J. E., Sanchez, S., Eastwood, J. P., & Freeman, M. P. (2023). Climatological predictions of the auroral zone locations driven by moderate and severe space weather events. Scientific Reports, 13(1), 779. https://doi.org/10.1038/s41598-022-25704-2
Malone-Leigh, J., Campanyà, J., Gallagher, P. T., Hodgson, J., & Hogg, C. (2024). Mapping geoelectric field hazards in Ireland. Space Weather, 22, e2023SW003638. https://doi.org/10.1029/2023SW003638
Mannucci, A.J. (2010) "Global Ionospheric Storms," White Paper submitted to the Space Studies Board of the US National Research Council for its 2010 “decadal survey” in solar and space physics (heliophysics). http://tinyurl.com/zsyz5ey
Marqué, C., Klein, K. L., Monstein, C., Opgenoorth, H., Pulkkinen, A., Buchert, S., ... & Thulesen, P. (2018). Solar radio emission as a disturbance of aeronautical radionavigation. Journal of Space Weather and Space Climate, 8, A42. DOI: 10.1051/swsc/2018029
Marsden, P. L., Berry, J. W., Fieldhouse, P., & Wilson, J. G. (1956). Variation of cosmic-ray nucleon intensity during the disturbance of 23 February 1956. *J. Atmos. Terr. Phys.* 8, 278-281. doi: 10.1016/0021-9169(56)90135-0
Mateo-Velez, J.-C, A. Sicard, D. Payan, N. Ganushkina, N.P. Meredith, and I. Sillpanaa, (2018), Spacecraft surface charging induced by severe environments at geosynchronous orbit, *Space Weather*, doi:10.1002/2017SW001689
Maunder, E.W. (1900). The Royal Observatory Greenwich: A Glance at its History and Work. Reprinted by Cambridge University Press, 2013.
McBeath, A. (1999) Meteors, comets and millennialism, Journal of the IMO, 27;6, 318-326. Available on ADS with bibliographic code: 1999JIMO...27..318M
Medford, L. V., L. J. Lanzerotti, J. S. Kraus, and C. G. Maclennan (1989), Transatlantic Earth Potential Variations During the March 1989 Magnetic Storms, Geophys. Res. Lett., 16, 10, doi: 10.1029/GL016i010p01145.
Mekhaldi, F., Muscheler, R., Adolphi, F., Aldahan, A., Beer, J., McConnell, J. R., Possnert, G., Sigl, M., Svensson, A. & Synal, H.-A. (2015). Multiradionuclide evidence for the solar origin of the cosmic-ray events of AD 774/5 and 993/4. *Nature communications*, 6. doi:10.1038/ncomms9611
Meredith, N. P., R. B. Horne, J. D. Isles, and J. V. Rodriguez (2015), Extreme relativistic electron fluxes at geosynchronous orbit: Analysis of GOES E >2 MeV electrons, *Space Weather* 13, doi:10.1002/2014SW001143.
Meredith, N., Horne, R., Isles, J., Ryden, K., Hands, A. and Heynderickx, D. (2016a) Extreme internal charging currents in medium Earth orbit: Analysis of SURF plate currents on Giove-A, *Space Weather*, 14, 578–591. doi:10.1002/2016SW001404.
Meredith, N. P., R. B. Horne, J. D. Isles, and J. C. Green (2016b), Extreme energetic electron fluxes in low Earth orbit: Analysis of POES E > 30, E > 100 and E > 300 keV electrons, *Space Weather*, 14, 136–150, doi:10.1002/2015SW001348.
Meredith, N. P., R. B. Horne, I. Sandberg, C. Papadimitriou, and H. D. R. Evans (2017), Extreme relativistic electron fluxes in the Earth's outer radiation belt: Analysis of INTEGRAL IREM data, *Space Weather*, 15, 917–933, doi:10.1002/2017SW001651.
Meredith, N. P., Cayton, T. E., Cayton, M. D., & Horne, R. B. (2023). Extreme relativistic electron fluxes in GPS orbit: Analysis of NS41 BDD-IIR data. Space Weather, 21, e2023SW003436. https://doi.org/10.1029/2023SW003436
Mitchell, C. N., L. Alfonsi, G. De Franceschi, M. Lester, V. Romano, and A. W. Wernik (2005), GPS TEC and scintillation measurements from the polar ionosphere during the October 2003 storm, Geophys. Res. Lett., 32, L12S03, doi:10.1029/2004GL021644.
Miyake, F., K. Nagaya, K. Masuda, and T. Nakamura (2012), A signature of cosmic-ray increase in AD 774–775 from tree rings in Japan, *Nature* 486, 240-242, doi: 10.1038/nature11123.

Miyake, F., I. Usoskin and S. Poluianov, editors, (2020) Extreme Solar Particle Events: The Hostile Sun, IOP Publishing Ltd, Bristol, UK. doi: 10.1088/2514-3433/ab404a.
Muratore, G., Giannini, T., & Micheli, D. (2022). Solar radio emission as a disturbance of radiomobile networks. *Scientific Reports*, *12*(1), 9324. doi: 10.1038/s41598-022-13358-z
NASA (2011). Mitigating In-Space Charging Effects-A Guideline. NASA-HDBK-4002. https://standards.nasa.gov/standard/nasa/nasa-hdbk-4002.
National Grid (2021a). Electricity transmission, https://www.nationalgrid.com/uk/electricity-transmission/ (last accessed 5 Dec 2021)
National Grid (2021b). Electricity Ten-Year Statement at Appendix B of https://www.nationalgrideso.com/document/181706/download
Nevanlinna, H., Tenhunen, P., Pirjola, R., Annanpalo, J., & Pulkkinen, A. (2001). Breakdown caused by a geomagnetically induced current in the Finnish telesystem in 1958. *Journal of Atmospheric and Solar-Terrestrial Physics*, *63*(10), 1099-1103. https://doi.org/10.1016/S1364-6826(01)00021-9
Ngwira, C. M., A. Pulkkinen, F. D. Wilder, and G. Crowley (2013), Extended study of extreme geoelectric field event scenarios for geomagnetically induced current applications, *Space Weather* 11, 121–131, doi:10.1002/swe.20021.
Ngwira, C. M., A. A. Pulkkinen, E. Bernabeu, J. Eichner, A. Viljanen, and G. Crowley (2015), Characteristics of extreme geoelectric fields and their possible causes: Localized peak enhancements, *Geophys. Res. Lett.* 42, 6916–6921, doi:10.1002/2015GL065061.
Nikitina, L., L. Trichtchenko, and D. H. Boteler (2016), Assessment of extreme values in geomagnetic and geoelectric field variations for Canada, *Space Weather*, 14, 481–494, doi:10.1002/2016SW001386.
O'Brien, T. P., J. F. Fennell, J. L. Roeder, and G. D. Reeves (2007), Extreme electron fluxes in the outer zone, *Space Weather* 5, S01001, doi:10.1029/2006SW000240.
O'Brien, T. P. (2009) SEAES-GEO: A spacecraft environmental anomalies expert system for geosynchronous orbit, *Space Weather* 7, S09003, doi:10.1029/2009SW000473
O'Hare, P., Mekhaldi, F., Adolphi, F., Raisbeck, G., Aldahan, A., Anderberg, E., ... & Park, J. (2019). Multiradionuclide evidence for an extreme solar proton event around 2,610 BP (~ 660 BC). *Proceedings of the National Academy of Sciences*, 116, 5961-5966. doi: 10.1073/pnas.1815725116
Oliveira, D. M., Zesta, E., Schuck, P. W., & Sutton, E. K. (2017). Thermosphere global time response to geomagnetic storms caused by coronal mass ejections. *Journal of Geophysical Research: Space Physics*, 122, 10,762–10,782. https://doi.org/10.1002/2017JA024006
Oliveira, D. M., & Zesta, E. (2019). Satellite orbital drag during magnetic storms. *Space Weather*, 17, 1510–1533. https://doi.org/10.1029/2019SW002287
Oliveira, D. M., Zesta, E., & Nandy, D. (2025). The 10 October 2024 geomagnetic storm may have caused the premature reentry of a Starlink satellite. *Frontiers in Astronomy and Space Sciences*, 11, 1522139. https://doi.org/10.3389/fspas.2024.1522139
Oughton, E. J., Hapgood, M., Richardson, G. S., Beggan, C. D., Thomson, A. W. P., Gibbs, M., et al. (2018). A Risk Assessment Framework for the Socioeconomic Impacts of Electricity Transmission Infrastructure Failure Due to Space Weather: An Application to the United Kingdom. *Risk Analysis*. https://doi.org/10.1111/risa.13229
Owens, M.J., Barnard, L.A., Pope, B.J.S. et al. (2022) Solar Energetic-Particle Ground-Level Enhancements and the Solar Cycle. *Sol Phys* 297, 105 . https://doi.org/10.1007/s11207-022-02037-x
Quenby, J. J., Webber, W. (1959) Cosmic-ray geomagnetic cut-off rigidities and the Earth's magnetic field, *Phil. Mag.*, 4, 90-112. doi:10.1080/14786435908238229

Parker, W. E., & Linares, R. (2024). Satellite drag analysis during the May 2024 Gannon geomagnetic storm. *Journal of Spacecraft and Rockets*, 61(5), 1412-1416. https://doi.org/10.2514/1.A36164
Patterson, C. J., Wild, J. A., & Boteler, D. H. (2023a). Modeling the impact of geomagnetically induced currents on electrified railway signaling systems in the United Kingdom. *Space Weather*, 21, e2022SW003385. https://doi.org/10.1029/2022SW003385
Patterson, C. J., Wild, J. A., & Boteler, D. H. (2023b). Modeling "wrong side" failures caused by geomagnetically induced currents in electrified railway signaling systems in the UK. *Space Weather*, 21, e2023SW003625. https://doi.org/10.1029/2023SW003625
Patterson, C.J., Wild, J.A., Beggan, C.D. et al. Modelling electrified railway signalling misoperations during extreme space weather events in the UK. *Sci Rep* 14, 1583 (2024a). https://doi.org/10.1038/s41598-024-51390-3
Patterson, C. J. (2024b). Modelling the Impacts of Space Weather on UK Railway Signalling Systems (Doctoral dissertation, Lancaster University (United Kingdom)). https://doi.org/10.17635/lancaster/thesis/2317
Pinto Jayawardena, T., Buesnel, G., Mitchell, C., Boyles, R., Forte, B. and Watson, R., 2017. Towards Re-Creating Real-World Ionospheric Scintillation Events in a Spirent Simulator-Based Robust PNT Test Framework. In: The Institute of Navigation International Technical Meeting , 2017
Preston, J., Chadderton,C., Kaori,K. and Edmonds,C. (2015) Community Response in disasters: an ecological learning framework, *International Journal of Lifelong Education*, 34;6, 727-753. doi: 10.1080/02601370.2015.1116116
Preston, J., (2018). Grenfell Tower: Preparedness, Race and Disaster Capitalism. Palgrave: London.
Preston, J. and Firth, R., (2020). Coronavirus, Class and Mutual Aid in the United Kingdom. Palgrave: London.
Puchalska, M., Sihver, L., Sato, T., Berger, T. & Reitz, G. (2012) Simulations of Matroshka Experiment outside the ISS using PHITS. *Advances in Space Research*, 50, 489-495.
Pulkkinen, Antti, Emanuel Bernabeu, Jan Eichner, Ari Viljanen and Chigomezyo Ngwira (2015) Regional-scale high-latitude extreme geoelectric fields pertaining to geomagnetically induced currents. *Earth, Planets and Space* 67:93, doi: 10.1186/s40623-015-0255-6
Ranjan, A. K., Nailwal, D., Sunil Krishna, M. V., Kumar, A., & Sarkhel, S. (2024). Evidence of potential thermospheric overcooling during the May 2024 geomagnetic superstorm. *Journal of Geophysical Research: Space Physics*, 129, e2024JA033148. https://doi.org/10.1029/2024JA033148
Reeves, G., Colvin, T., Locke, J. et al. (2019). Next steps space weather benchmarks. IDA Group Report NS GR-10982. Institute for Defense Analyses, Washington DC, USA. December 2019.
Reitz, G., Berger, T., Bilski, P., Burmeister, S., Labrenz, J., Hager, L., Palfalvi, J. K., Hajek, M., Puchalska, M. & Sihver, L. (2010) Hamlet-Human Model Matroshka for radiation exposure determination of astronauts- Current status and results. 38th COSPAR Scientific Assembly, 3202.
Riley, P. (2012), On the probability of occurrence of extreme space weather events, *Space Weather* 10, S02012, doi: 10.1029/2011SW000734.
Riley, P., and Love, J. J. (2017), Extreme geomagnetic storms: Probabilistic forecasts and their uncertainties, *Space Weather*, 15, 53– 64, doi:10.1002/2016SW001470.
Rishbeth, H., Shea, M. A., Smart, D. F., 2009, "The solar-terrestrial event of 23 February 1956," *Advances in Space Research* 44, 1096-1106. doi: 10.1016/j.asr.2009.06.020

Roberts, P.H. (2015) Theory of the Geodynamo, in Treatise on Geophysics (Second Edition), 57-90, Editor: Gerald Schubert, published by Elsevier, doi: 10.1016/B978-0-444-53802-4.00144-5.
Rodger, C. J., Mac Manus, D. H., Dalzell, M., Thomson, A. W. P., Clarke, E., Petersen, T., … Divett, T. (2017). Long-term geomagnetically induced current observations from New Zealand: Peak current estimates for extreme geomagnetic storms. *Space Weather*, 15. Doi: 10.1002/2017SW001691
Rodger, C. J., Clilverd, M. A., Mac Manus, D. H., Martin, I., Dalzell, M., Brundell, J. B., et al (2020). Geomagnetically Induced Currents and Harmonic Distortion: Storm-time Observations from New Zealand. Space Weather, 18, e2019SW002387. Doi: 10.1029/2019SW002387
Rogers, N. C., Wild, J. A., Eastoe, E. F., Gjerloev, J. W., & Thomson, A. W. (2020). A global climatological model of extreme geomagnetic field fluctuations. Journal of Space Weather and Space Climate, 10, 5. Doi: 10.1051/swsc/2020008
Roederer, J. G. (1970), Dynamics of Geomagnetically Trapped Radiation, Springer, New York, doi:10.1007/978-3-642-49300-3.
Roederer, J. G., & Lejosne, S. (2018). Coordinates for representing radiation belt particle flux. Journal of Geophysical Research: Space Physics, 123, 1381– 1387. Doi: 10.1002/2017JA025053
Rogers, N.C., and F. Honary (2015), Assimilation of Real-time Riometer Measurements into Models of 1-30 MHz Polar Cap Absorption, J. Space Weather and Space Climate, **5**, A8 DOI:10.1051/swsc/2015009, 2015.
Rogers, N. C., F. Honary, J. Hallam, A.J. Stocker, E.M. Warrington, D.R. Siddle, D. Danskin and B. Jones, "Assimilative Real-time Models of HF Absorption at High Latitudes", Proc. 14th International Ionospheric Effects Symposium, Alexandria, VA, USA, 12-14 May 2015. (Paper 48), 2015. Available online: http://ies2015.bc.edu/wp-content/uploads/2015/05/048- Rogers-Paper.pdf. Also submitted to Radio Sci., Sept. 2015 (IES 2015 Special Issue).
Ryden, K.A. et al., (2008) Observations of Internal Charging Currents in Medium Earth Orbit," IEEE Transactions on Plasma Science 36, 2473-2481. doi: 10.1109/TPS.2008.2001945
Ryden, K.A. and A. D. P. Hands. (2017) Modeling of Electric Fields Inside Spacecraft Dielectrics Using In-Orbit Charging Current Data, I*EEE Trans. Plasma Sci.* 45, 1927-1932. doi: 10.1109/TPS.2017.2665622
Sanders, R. (1961). Effect of terrestrial electromagnetic storms on wireline communications. IRE Transactions on Communications Systems, 9(4), 367-377. Doi: 10.1109/TCOM.1961.1097724
Sauer, H. H., and D. C. Wilkinson. Global mapping of ionospheric HF/VHF radio wave absorption due to solar energetic protons. Space Weather, 6, S12002, 2008, DOI: 10.1029/2008SW000399.
Sciencewise (2014) Space Weather: Public Dialogue, STFC, BIS: London. http://www.sciencewise-erc.org.uk/cms/space-weather-dialogue.
Schlüter, S., & Hoque, M. M. (2020). An SBAS integrity model to overbound residuals of higher-order ionospheric effects in the Ionosphere-free linear combination. Remote Sensing, 12(15), 2467. https://doi.org/10.3390/rs12152467
Schumer, E. A. Improved modeling of midlatitude D-region ionospheric absorption of high frequency radio signals during solar x-ray flares. Ph.D. dissertation, AFIT/DS/ENP/09-J01, p.49, United States Air Force, Wright-Patterson Air Force Base, Ohio, USA, June 2009.
Shprits, Y., D. Subbotin, B. Ni, R. Horne, D. Baker, and P. Cruce (2011), Profound change of the near-Earth radiation environment caused by solar superstorms, *Space Weather* 9, S08007, doi:10.1029/2011SW000662.

Sihver, L., Ploc, O., Puchalska, M., Ambrožová, I., Kubančák, J., Kyselová, D., & Shurshakov, V. (2015). Radiation environment at aviation altitudes and in space. Radiation protection dosimetry, 164(4), 477-483. Doi: 10.1093/rpd/ncv330
Siscoe, G. L., Crooker, N. U., & Clauer, C. R. (2006). Dst of the Carrington storm of 1859. Advances in Space Research, 38(2), 173–179. Doi: 10.1016/j.asr.2005.02.102
Skone, S. (2000) Impact of Ionospheric Scintillation on SBAS Performance, ION GPS 2000, Salt Lake City, Utah, 284-293.
Smith, P.M. (1990). Effects of geomagnetic disturbances on the national grid system. Universities Power Engineering Conference (UPEC).
Spurný, F., Ploc, O., & Dachev, T. (2007). On the neutron contribution to the exposure level onboard space vehicles. Radiation protection dosimetry, 126(1-4), 519-523. Doi: 10.1093/rpd/ncm104
Sutton, E.K, J. M. Forbes, and R. S. Nerem (2005) Global thermospheric neutral density and wind response to the severe 2003 geomagnetic storms from CHAMP accelerometer data, *J. Geophys. Res*. 110, A09S40, doi:10.1029/2004JA010985
Sutton, E. K., J. M. Forbes, and D. J. Knipp (2009), Rapid response of the thermosphere to variations in Joule heating, *J. Geophys. Res.*, 114, A04319, doi:10.1029/2008JA013667.
Thomson, A. W. P., E. B. Dawson, and S. J. Reay (2011), Quantifying extreme behavior in geomagnetic activity, *Space Weather*, 9, S10001, doi: 10.1029/2011SW000696.
Tsurutani, B. T., W. D. Gonzalez, G. S. Lakhina, and S. Alex (2003), The extreme magnetic storm of 1–2 September 1859, *J. Geophys. Res.* 108, 1268, doi:10.1029/2002JA009504, A7.
Tylka, Allan J. And Dietrich, William (2009) "A New and Comprehensive Analysis of Proton Spectra in Ground-Level Enhanced (GLE) Solar Particle Events" Proceedings of the 31st International Cosmic Ray Conference (Łódź), 7-15.
Vette, J.I. (1991). The AE-8 Trapped Electron Model Environment. NASA report NSSDC/WDC-A-R&S 91-24. https://ntrs.nasa.gov/search.jsp?R=19920014985. Accessed 2 July 2020.
Warrington, E. M., N. Y. Zaalov, J. S. Naylor, and A. J. Stocker (2012), HF propagation modeling within the polar ionosphere, Radio Sci., 47, RS0L13, doi:10.1029/2011RS004909.
Watermann, J. (2007) The Magnetic Environment – GIC and other ground effects, in: Lilensten, J. (Ed.), Space Weather – Research towards applications in Europe. Springer, Dordrecht, pp. 269-275, 2007.
Wintoft, P., Viljanen, A., and Wik, M. (2016) Extreme value analysis of the time derivative of the horizontal magnetic field and computed electric field, *Ann. Geophys.* 34, 485-491, doi: 10.5194/angeo-34-485-2016.
Xapsos, M. A., G. P. Summers, J. L. Barth, E. G. Stassinopoulos, and E. A. Burke (1999), Probability Model for Worst Case Solar Proton Event Fluences, *IEEE Trans. Nucl. Sci.* 46, 1481-1485
Xapsos, M. A., G.P. Summers, J.L. Barth, E. G. Stassinopoulos and E.A. Burke (2000) "Probability Model for Cumulative Solar Proton Event Fluences", *IEEE Trans. Nucl. Sci*. vol. 47, no. 3, June 2000, pp 486-490. Doi: 10.1109/23.856469
Zhang, S., Wimmer-Schweingruber, R. F., Yu, J., Wang, C., Fu, Q., Zou, Y., ... & Quan, Z. (2020). First measurements of the radiation dose on the lunar surface. Science Advances, 6(39), eaaz1334. Doi: 10.1126/sciadv.aaz1334

12 Appendix 1: Interrelationships between effects

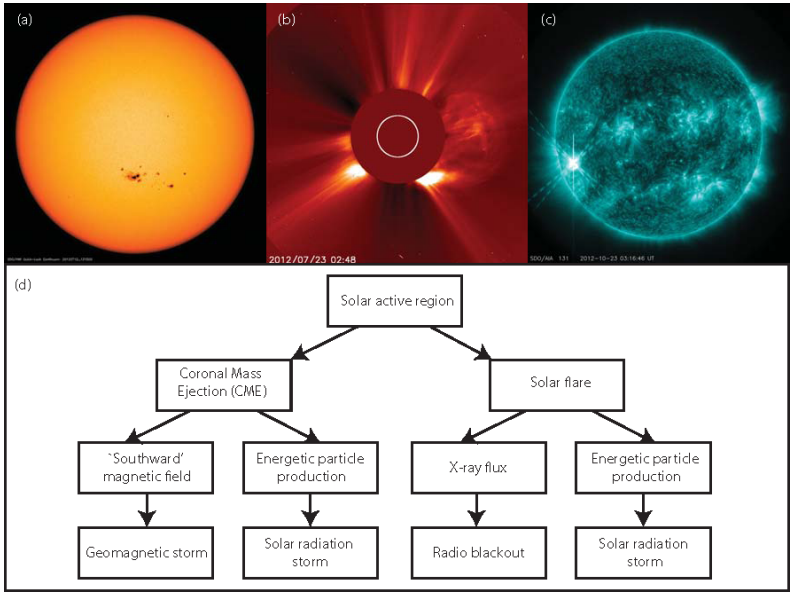

The Sun is essentially the ultimate source of space weather at Earth as illustrated in Figure 1 (Eastwood et al., 2017). Large sunspot groups on the solar disk (panel a) indicate the presence of active regions in the solar atmosphere which are the typical site of *coronal mass ejections* (panel b) and *solar flares* (panel c). These two solar phenomena can interact with the Earth's magnetic field in space (magnetosphere), ionosphere, and atmosphere to generate geomagnetic storms, solar radiation storms, and radio blackouts.

The duration of an interval of severe space weather is expected to depend on its likelihood, with rare severe events lasting longer in time. Studies by Eastwood et al. (2018) and Oughton et al. (2018) examining power grid economic impact in Europe and the UK respectively have made use of 1-in-10 year, 1-in-30 year, and 1-in-100 year scenarios based on the October 2003, March 1989, and 1859 Carrington periods respectively. Figure 2 shows the expected duration of each scenario and illustrates the potential complexity of an interval of extended space weather risk, which could for several weeks.

Figure 3 outlines many of the most important associations between space weather effects and system impacts such as those described in this document. Many space weather effects will occur close together in time as they have a common origin in solar phenomena such as coronal mass ejections. Given the expected complexity as illustrated in Figure 2, it is reasonable to expect that different systems will experience interacting adverse impacts causing unpredictable and cascading failures.

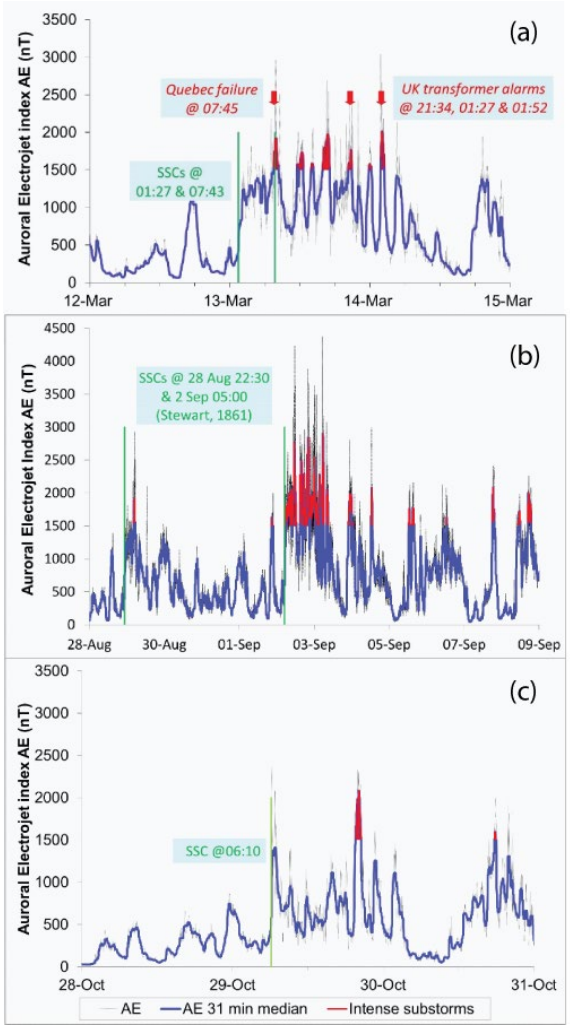

Figure 2 Candidate scenarios for the duration and complexity of 1-in-30 (panel a), 1-in-100 (panel b), and 1-in-10 year events (panel c). Figures show the time series of the AE index (used to characterize auroral activity associated with risk to power grids) with a 31-min running median trace overlaid (blue). Intervals of intense activity representing risk to power grids are shown in red. SSC refers to sudden storm commencement. (Reproduced from Eastwood et al., Space Weather, 2018 https://doi.org/10.1029/2018SW002003, Figure 1; see also Oughton et al. 2018).

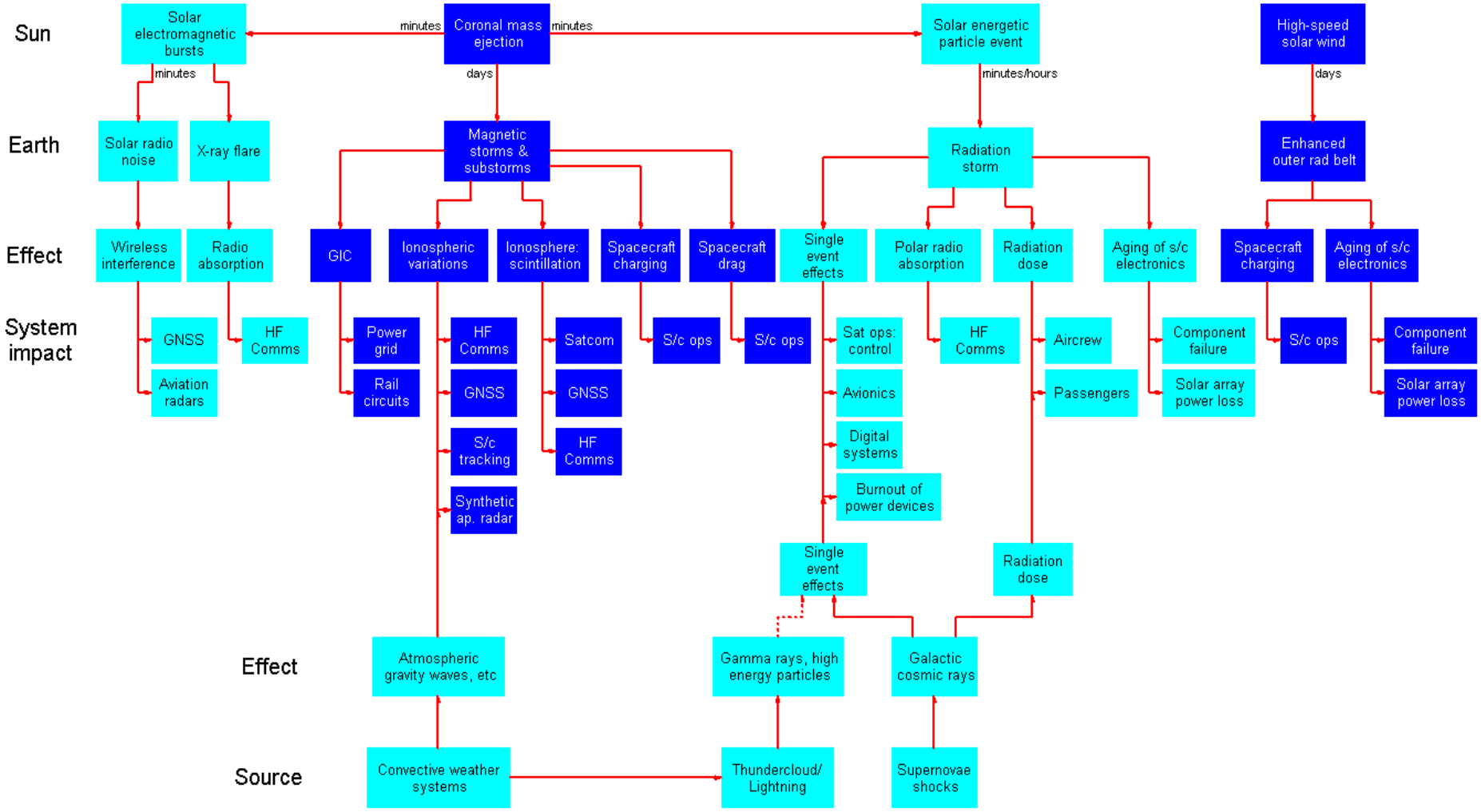

Figure 3 The association between the physical drivers of space weather and downstream system impacts.

13 Appendix 2. Space Weather: potential 'worst case' public behaviour impacts: note by John Preston.

Introduction

Public behaviour after a severe space weather event is difficult to predict as the infrequency of such events does not give us a baseline. Infrastructure failure following an extreme event may result in behaviours such as public disorder or stockpiling that might be expected in a major crisis. This depends on the scale of the event. The 1989 solar storm which caused a blackout in Toronto, closing schools and businesses, did not result in notable public behaviour anomalies but the impact on the electricity grid was short lived.

Because of the source of space weather events they might be subject to conspiracy theories and rumours that reject scientific explanations. Very rarely, cult groups have used solar events as a 'sign' to take action in terms of mass suicides or violent actions. The four potential impacts provided below would only be seen in a worst case scenario.

Rejection of scientific understanding in favour of conspiracy / rumour

Severe space weather is a low probability, high impact event where there is little public understanding. A telephone survey of 1,010 adults in England and Wales conducted in 2014 found that 46% had never heard of space weather and an additional 29% had heard of it but know almost nothing about it. 35% of respondents would be more concerned about a power cut in their area caused by space weather when compared to other causes (Sciencewise, 2014). Scientific understanding of space phenomena can be undermined by conspiracy theories which may propagate online through the echo chamber effects of social media. For example, online rumours concerning the existence of a so called 'Planet X' or 'Nibiru' which will collide with earth have circulated online since 1995 despite the absence of scientific evidence (Kerr, 2011). *A worst case scenario would be that lack of existing knowledge of space weather and the propagation of rumour and conspiracy on-line (perhaps involving bad state actors) would increase public anxiety around the event.*

Reframing of the event with negative consequences for social cohesion

A recent comparative survey of public behaviour in disasters and emergencies which impact at regional or national level showed that in most cases communities will usually react in ways with neutral or positive impacts on social cohesion (Preston et al, 2015). In the Coronavirus pandemic there were many examples of spontaneous mutual aid and volunteering even without Government action (Preston and Firth, 2020). However, in some cases communities will react negatively to official help and advice and politicise the event. This community behaviour in disasters, known as *reframing*, may occur in a severe space weather event particularly if communities consider that the official response is not equitable. For example, if power is restored to communities in a way that is perceived to be unfair then it is likely that there will be negative political consequences that may result in demonstrations or public disorder. Inequity in preparation or response to an event is likely to be a major catalyst for protests (Preston, 2018).

Mitigating against this, unpredictable or novel emergencies will not usually lead to political outrage as long as the public are made aware of the reasons for the event (but see point 1 above). *A worst case scenario would be that there is public disorder in communities where the government response is seen to be inadequate*.

Stockpiling (sometimes called 'panic buying')

Stockpiling is a rational behaviour in disasters and emergencies and is not a problem as long as retail stocks and supply chains are not compromised. Goods that are usually stockpiled are petrol, bottled water and canned goods. If people consider that stocks and supply chains may be compromised in the future, or that they need excess supplies at home for an anticipated event, they may increase demand to the extent that current supply cannot meet demand. This can become a self-fulfilling prophecy as in the Coronavirus pandemic when in March 2020 many supermarkets were experiencing shortages. Fear of shortages leads to stockpiling which in turn leads to shortages that exacerbate demand through 'panic buying' resulting in shortages. Prices may rise rapidly, queuing may occur, stocks can be depleted and (rarely) some individuals may resort to theft to obtain supplies. Supply chains in the UK are lean (little stock is held) and are particularly vulnerable to panic buying in a crisis (House of Lords Scientific Committee, 2005). *A worst case scenario would be widespread panic buying which would compromise supply chains and lead to inefficiencies such as queuing for petrol.*

Millenarianism

Millenarianism refers a view of certain religious sects, or individuals, who consider that certain events are a sign that the world is coming to an end. These events are often linked to space events such as comets (McBeath, 2011) and pseudo-scientific concepts such as changes in 'galactic alignment' or cataclysmic 'pole shifts'. Sometimes religious cults use space events as a justification for mass suicides or violent events. For example, the 1999 suicide of 31 members of the 'Heaven's Gate' cult in San Diego, California was planned after their observations of the Hale-Bop comet in 1997 (they believed a spacecraft trailing the comet would take them from earth). 53 members of The Order of the Solar Temple, who worship the Sun, died in Switzerland in 1994. Many of these deaths were as a result of shooting and stabbing of their own members as well as from suicide. The Order of the Solar Temple is still in existence. Such events are difficult to predict but may coincide with a solar event such as severe space weather. *A worst case scenario would be a mass suicide, or other violent event, initiated by a cult group.*